Report 11, 1993

A 3-D NATURAL STATE MODELLING AND RESERVOIR ASSESSMENT FOR THE BERLIN GEOTHERMAL FIELD IN EL SALVADOR, C.A.

Manuel Ernesto Monterrosa Vasquez,
UNU Geothermal Training Programme,
Orkustofnun - National Energy Authority,
Grensasvegur 9,
108 Reykjavik,
ICELAND

Permanent address:
Comisión Ejecutiva Hidroeléctrica del Rio Lempa,
Superintendencia de explotación geotérmica,
Gerencia de GEOCEL, Col. Utila Nueva San Salvador,
La Libertad, Apartado postal 2669,
EL SALVADOR, C.A.

ABSTRACT

Twenty-five years have passed since geothermal research and drilling were activated in the Berlin geothermal field, El Salvador. In this report, a brief description is given on the surface exploration carried out in the area, and the six deeper wells drilled. Evaluation of formation temperatures and pressures are given.

The results of these studies are unified into a single, conceptual model of the geothermal system. An upflow zone of ≥ 300°C is assumed underneath the Berlin caldera. The fluid flows laterally towards northeast into the present wellfield, where the flow changes direction towards the northnorthwest. The reservoir is of two layers, a shallow one of 200-230°C at sea level and a deep one of 270-290°C at -1000 m a.s.l. All of the reservoir volume seems to be in a single-phase, liquid condition. The deeper reservoir is productive.

A study on interference data reveals permeabilities in the order of 50-100 mD. High storativity values are also evident. A wellbore simulation study indicates that the Berlin wells flash down to their feedzones, during production, and some distance into the reservoir. Enthalpy changes are, however, still negligible.

The conceptual reservoir model and the production data were simulated in a 3-dimensional grid, using the TOUGH simulator. A satisfactory match was obtained for the measured and the calculated data. The high reservoir storativity was presumed to be due to a large volume of the single-phase liquid reservoir (60-80 km^3). This may be unrealistic, suggesting that a free surface storativity, due to boiling at shallow depths, should also be considered.

The numerical reservoir model is assumed to be inadequate for performance predictions, due to limited production data available to simulate. However, a quantitative study of the production capacity, by using volumetric assessment and some random distribution in the reservoir properties, suggest that up to 60 MW_e may be available for a 30 year generation period.

TABLE OF CONTENTS

LIST OF FIGURES

Page

LIST OF TABLES

1. INTRODUCTION

The Berlin geothermal field is located 5 km from Berlin city in the eastern part of El Salvador in Central America. The first evaluation of geothermal energy was carried out in 1966 in a project between the United Nations Development Programme (UNDP) and the Comisión Ejecutiva Hidroeléctrica del Rio Lempa (CEL). During this stage well TR-1 was drilled. Downhole surveys revealed a commercially exploitable geothermal reservoir of temperatures close to 230°C at 1350 m. However, this well presents low permeability.

From 1978 to 1981, five additional wells were drilled: TR-2, TR-3, TR-4, TR-5 and TR-9. All except TR-4 are very good producers (40-80 kg/s of 1300 kJ/kg).

A feasibility study was carried out by Electroconsult (ELC) in 1981. Due to political problems in El Salvador, this project was kept in stand-by position. The geothermal project was reactivated in 1990-1991 when CEL installed two back pressure units of 5 MW_e each, using TR-2 and TR-9 as producers and TR-1 and TR-6 for reinjection. Well TR-6 was scheduled to be completed in 1991, but due to a blow-out explosion at 150 m depth, further drilling was terminated and the well cemented. For lack of reinjection wells, CEL decided to use TR-9 for reinjection and only one power unit went on line. In May 1993 the electricity production at the Berlin power plant was stopped and further production is to be halted until new injection wells are available.

As part of a feasibility study CEL is questioning the size of a new condensing power plant and furthermore an optimum development strategy for the Berlin geothermal field. Reservoir engineering studies will play a major role in this decision making.

The following report presents a reservoir simulation study for the Berlin field. It is part of the 1993 UNU Geothermal Training Programme at Orkustofnun, National Energy Authority, Reykjavik, Iceland during April to October 1993.

An outline is given of the reservoir geology, an evaluation of reservoir pressure and formation temperature is made, and a conceptual reservoir model presented. The conceptual model is, furthermore, simulated by a 3-dimensional numerical grid and, finally, a performance study is made using three different approaches of volumetric assessment.

2. GEOLOGICAL OUTLINE OF THE BERLIN FIELD

2.1 Geology and hydrothermal alteration

The Berlin geothermal field is located in the northwestern part of the Tecapa-Berlin volcanic structure. The area is very active tectonically due to the subduction of the Cocos Plate into the Caribbean Plate. The field is associated to a nearby Quaternary caldera, which is supposed to be an active heat source for the Berlin geothermal field (ELC, 1993). Figure 1 gives an overview of the Berlin field.

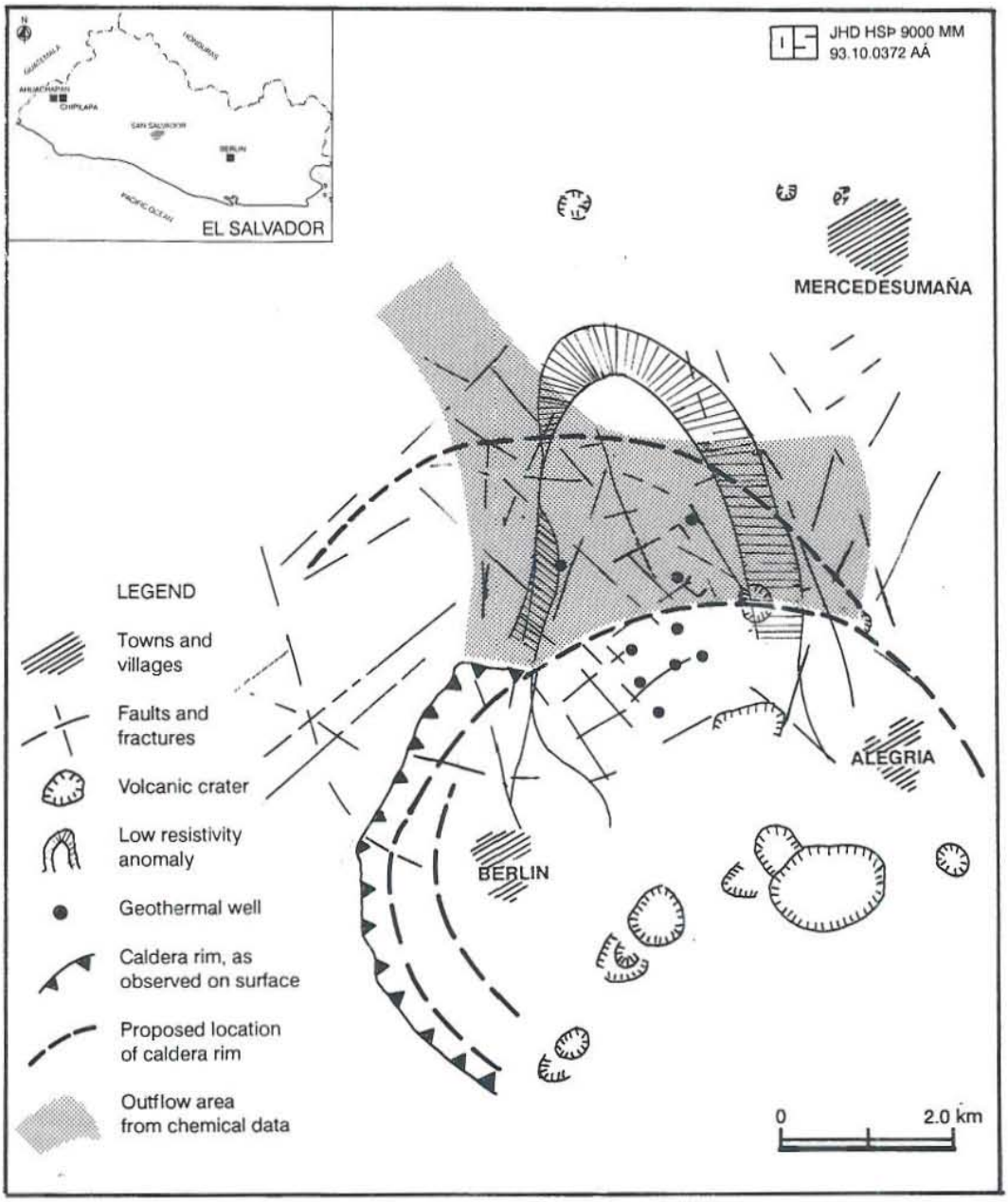

FIGURE 1: An overview of the Berlin geothermal field

The geology of the Berlin field has been divided into three main structures (CEL, 1990):

a) Annular faults formed by a caldera collapse.
b) Regional fault system with NE-SW orientation, perhaps related to a central graben.
c) Transverse faults with NNW-SSE orientation, perhaps related to the caldera collapse.

The NNW-SSE faults are younger and seem to be more active tectonically than the NE-SW faults. Several hot springs and fumaroles are aligned to these faults. A study of hydrothermal alteration in the Berlin wells indicates that some fluid is moving along the elder NE-SW faults, but geothermal fluids are also believed to be moving along the northnorthwesterly directed faults (ELC, 1982).

The rocks of the Berlin area are volcanic type with composition from basic to intermediate and intermediate-acid; some pyroclastic deposits are observed on the surface. Analysis of well cuttings show a succession of horizontal lavas and tuff layers inside the lithological strata. These structures are believed to allow fluid movement; hence relatively high horizontal permeabilities are expected in the region. The geothermal reservoir itself is mainly composed of highly fractured andesite rocks.

The classification still used by CEL for the hydrothermal alteration presents prophillitic face into the geothermal reservoir below the caprock with alteration temperatures of 220 to 300°C in good agreement with measured data in the wells. This face is characterized by the presence of minerals like epidote and wairakite; whereas the argillitic face is characterized with minerals like hematite.

Some main properties of core samples and cuttings have been analyzed in CEL's labs. The data show porosity of 10.7% ± 5.7%, bulk density of 2620 ±13 kg/m^3 and matrix rock permeability between 0.05 and 0.3 mD (ELC, 1993).

2.2 Geophysical studies

The available geophysical data from the Berlin field is quite limited and consist mainly of resistivity and gravity surveys and some heat flow measurements. The gravity data seems to be of low quality and is therefore not applicable (ELC, 1993).

During 1977 a resistivity survey was carried out in the Berlin field using a 0.3 Hz DC transmitter. A total of 78 Schlumberger soundings were carried out with current electrode spacing up to AB/2=3000 m. However, at electrode spacing AB/2 larger than 1000 m, an electromagnetic effect disturbs the data. This erroneous effect is due to the current transmitter used in the survey. An updated analysis was presented by the 1993 report (ELC, 1993), where a reinterpretation of the whole data was made. According to this study a low resistivity layer (10-25 Ωm) is observed at 100-400 m depth with a NNW-SSE direction; and high resistivity layers (100-200 Ωm) on the western and the eastern sides of the present wellfield (Figure 1). These structures may present some impermeable boundaries in these regions. Otherwise limited results were obtained due to the data quality.

Correlation of downhole and resistivity data indicates that the low resistivity anomaly is caused by a shallow aquifer in the wellfield. Resistivity data at greater depths than -500 m a.s.l. is not available.

2.3 Geochemical studies

Generally, the geothermal fluids discharged from the Berlin reservoir are classified as sodium-chloride type with neutral pH and intermediate chloride content (6000 ppm). The gas concentration is relatively low (gas/steam ratio less than 150) and the salinity is between 7000 and 12000 ppm.

The chemical analysis identifies three types of geothermal aquifers (CEL, 1991):

a) A low salinity (1600 ppm), shallow aquifer at depths between 200 and 300 m a.s.l.
b) An intermediate saline aquifer (6600 ppm) at sea level.
c) A deeper saline aquifer (8000-12000 ppm) at a depth of -800 to -1200 m a.s.l.

The chemical composition (NH_3, B, H_2) of fluids taken from fumaroles and hot springs indicates that the heat source is located beneath the Tecapa volcano and that the main flow of the geothermal fluid follows a NNW-SSE direction along faults, in good agreement with the resistivity survey (Figure 1).

Several ratios for chemical species (CO_2/H_2S) indicate that the El Hoyon fumarole is the most representative for thermal discharge from the reservoir (CEL, 1991), indicating location close to the upflow of the system (to the southern and southwestern side of the present wellfield). However, the fumaroles located to the northern part of the wellfield, like El Trujillo, also indicate relatively high temperatures, perhaps related with shallow aquifers of lateral flow.

The geochemical studies show that a special emphasis must be made on reinjection and operating pressure of wells. This has to do with necessary disposal of contaminated water, but also with silica scaling in production and injection wells. This must be taken into account in later simulation studies.

3. EVALUATION OF THE BERLIN RESERVOIR

3.1 General information on wells

Geothermal drilling in the Berlin area was initiated in 1968 as a part of a UNDP regional programme. At that time three wells were drilled. Two of them are shallow, PEBL-1 and PEBL-2 (400-500 m deep). The third well, TR-1, was drilled to 1460 m. This well intersected a geothermal reservoir with temperatures close to 230°C at 1350 m. Production rates from the well are, however, low due to low permeability in the vicinity.

During 1978 to 1981, five additional wells were drilled TR-2, TR-3, TR-4, TR-5, and TR-9. All of them, except well TR-4, present high reservoir temperatures and very good production characteristics. During the TR-4 completion a fishing tool became stuck in the well, perhaps preventing discharge from it.

Table 1 gives an overview of the PEBL and TR wells in Berlin and Figure 2 shows the location of these wells (CEL, 1993).

TABLE 1: An overview of wells in the Berlin area

Well	Drill date		Location		Well design			Depth (m)	Elevation (m a.s.l)
	From	To	N-S (m)	E-W (m)	Casing 9 5/8"	Open hole 8 1/2"	Liner 7 5/8"		
PEBL1	1960	1960	266500	552500	-	-	-	525	700
PEBL2	1960	1960	267500	551500	-	-	-	400	500
TR-1	Jul 7, 68	Aug 20,68	267333	552860	0-325	750-1458	315-750	1458	552.8
TR-2	Jan 14,78	Jun 2,78	266276	552802	0-746	-	715-1903	1903	752
TR-3	Apr 24,79	Oct 30,79	266413	553129	0-1511	-	1474-2296	2300	760.8
TR-4	Jan 23,80	Jul 8,80	266097	552405	0-1302	1302-2150	2150-2293	2379	767.3
TR-5	Jan 30,81	Jul 4,81	265744	552606	0-1267	-	1242-2079	2086	840
TR-9	Sep 4,80	Dec 28,80	266726	552825	0-1142	-	1277-2298	2298	649.2

Notes: Well TR-4 has at the middle part intermediate 8 1/2" open hole and at the deeper part 143 m of 9 5/8" slotted liner both due to technical problems during the completion.
Well TR-1 has an obstruction at 634 m since 1980, perhaps due to rocks inside the well.

The Berlin wellfield is approximately 1.5 km^2 in area extent. In order to initiate discharge, all wells except TR-1 and TR-3 need to be compressed by air. All of the deep wells intersect their main feedzones close to -1000 m a.s.l. and the maximum bottomhole temperatures are close to 300°C.

3.2 Evaluation of formation temperatures and pressures

Well TR-1: Figures 3 and 4 show downhole temperature and pressure profiles in well TR-1, collected before April 1978 when an obstruction fell into the well at 634 m depth. These profiles are taken to represent the formation temperature and pressure of this well. The temperature profile is of a gradient type with signs of convective zones from sea level to -300 m a.s.l., and possibly another narrow one at -400 m a.s.l. The deeper part of the well shows a conductive and impermeable layer. No warm-up data is available for this well.

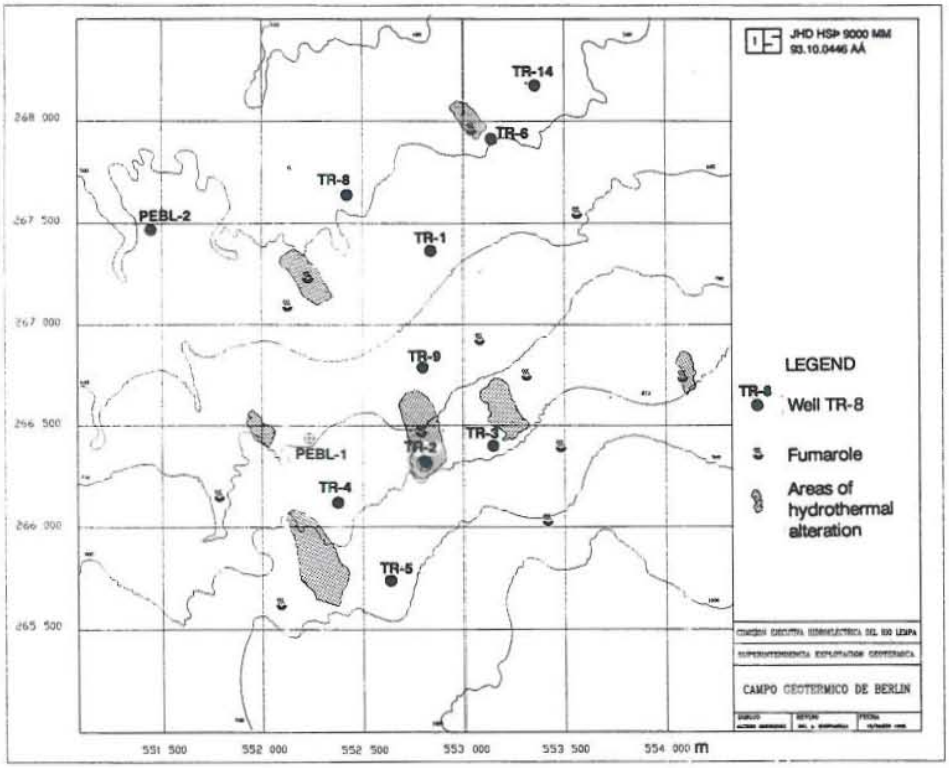

FIGURE 2: Location of wells in the Berlin field

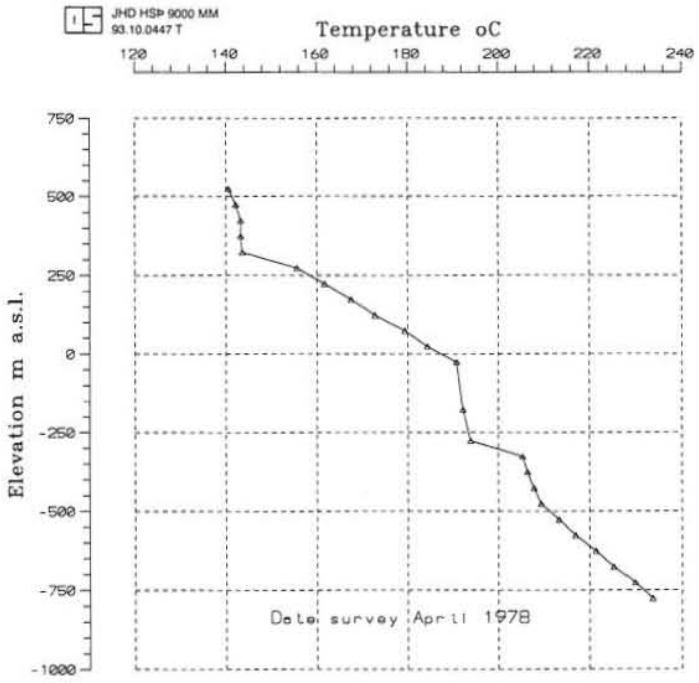

FIGURE 3: The formation temperature of TR-1

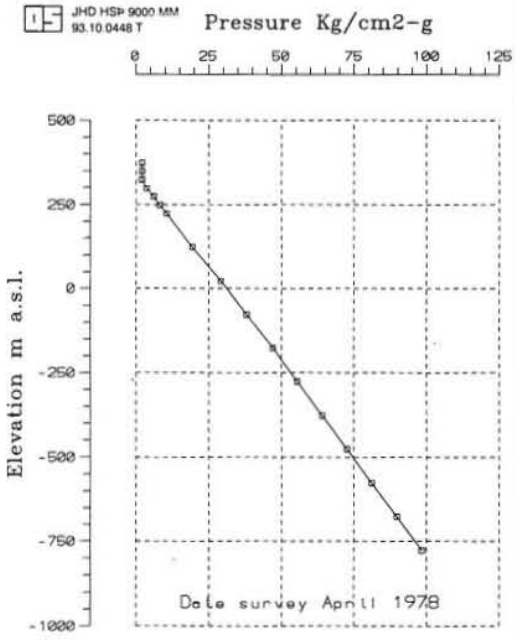

FIGURE 4: Pressure survey, well TR-1

Well TR-1 was used for injection during February 1992 to May 1993, therefore no reliable temperature surveys are available for a more detailed analysis of the formation temperature.

The pressure profile reflects a hydrostatic gradient from 300 m a.s.l. to the bottom of the well. This profile is taken to be in equilibrium with the total length of the open hole, since no internal flow occurs in it.

Well TR-2: This well is the best producer in the Berlin area. The main feedzones are of high temperatures and the well is providing close to 90 kg/s at 1350 kJ/kg enthalpy and 10 bar-a wellhead pressure. Figure 5 shows temperature measurements carried out during the warm-up period and Figure 6 shows some temperature surveys conducted after the well's first flow test. The figures show a temperature close to 300°C at -1000 m a.s.l. depth and a temperature reversal is evident at the bottom of the well.

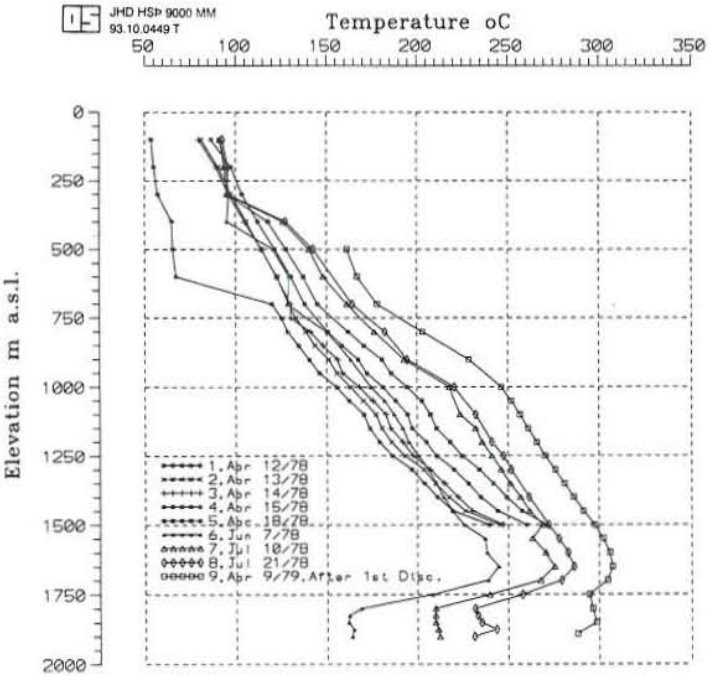

FIGURE 5: Temperature profiles collected during warm-up of well TR-2

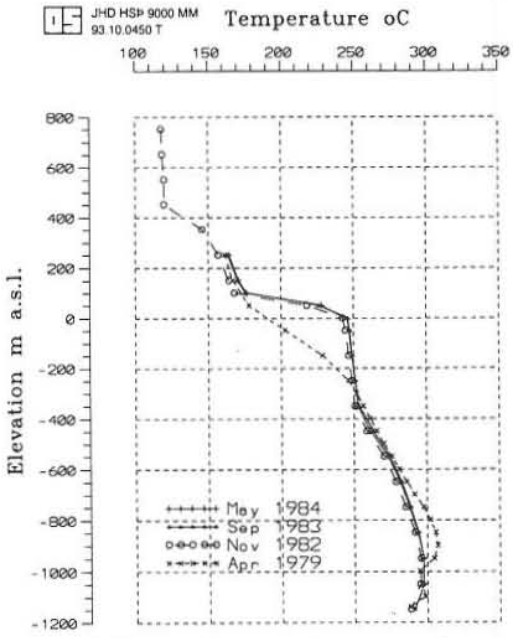

FIGURE 6: Temperature profiles in well TR-2 after its first discharge

The uppermost 360 m of the well's liner are unslotted, thus some internal flow takes place between the casing shoe and the solid part of the liner during shut-in conditions. This effect is evident in TR-2 after the first flow test, carried out in March 1981, and is seen as a knee in the downhole temperature at 100 to -300 m a.s.l. (Figure 6). Besides this, well TR-2 seems to be of a conductive gradient type down to the permeable zone at -700 to -1000 m a.s.l.; the temperature reversal indicates horizontal flow in that depth interval.

Figures 7 and 8 show several pressure profiles collected in TR-2; pivot point analysis shows that the main feedzone is located between -1000 and -1200 m a.s.l. with an initial pressure close to 120 kg/cm^2-g at -1000 m a.s.l. The water level during shut-in conditions is located at 300 m depth and all the wellbore fluid is in overpressurized liquid condition.

Pressure and temperature surveys carried out in TR-2 after 1.5 years of discharge from Feb 1992 to May 1993 show negligible changes in the downhole pressure and temperature.

Well TR-3: Figures 9 and 10 show selected temperature and pressure logs in well TR-3. During its warm-up a rapid thermal recovery occurred at +300 to 0 m a.s.l. with a final temperature close to 200°C. Another peak in temperature is seen at -400 to -600 m a.s.l. After several flow tests

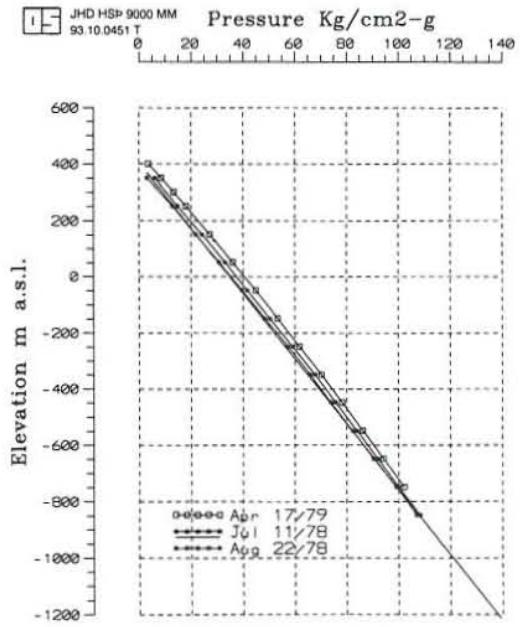

FIGURE 7: Pressure data in well TR-2 prior to discharge

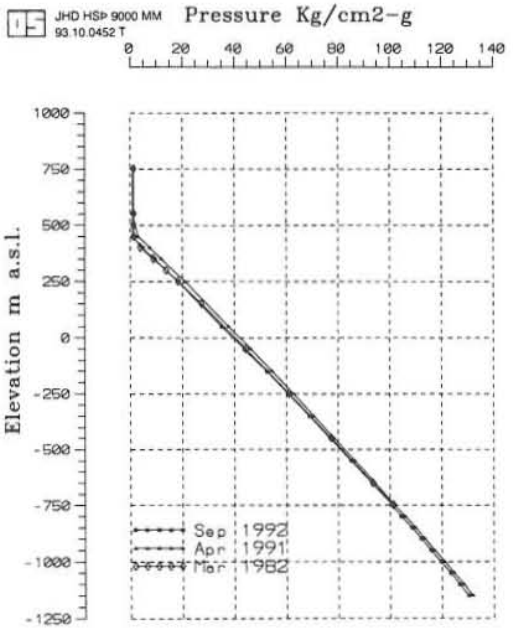

FIGURE 8: Pressure data in well TR-2 after discharge

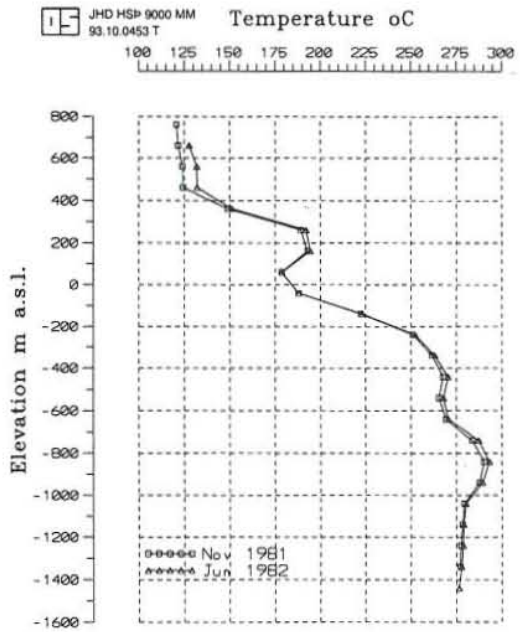

FIGURE 9: Temperature profiles collected in well TR-3

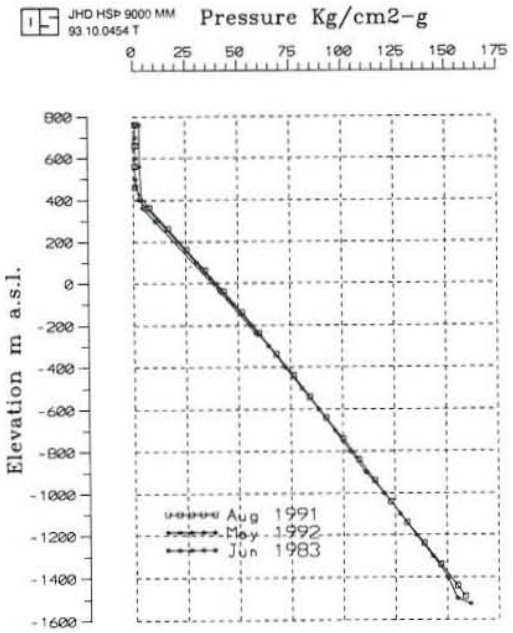

FIGURE 10: Pressure profiles collected in well TR-3

the well warmed up until stable conditions were obtained. The maximum temperature is close to 290°C located at -800 m a.s.l. A temperature reversal, similar to that in TR-2, is seen in the lowest part of well TR-3.

The pressure data in Figure 10 indicates that the pivot point and, hence, the main feedzone is located at -900 m a.s.l. with an initial pressure close to 114 kg/cm^2-g. Repeated pressure surveys through several years present no significant changes, despite substantial discharge from wells in the vicinity.

Well TR-4: Figures 11 and 12 show downhole temperature and pressure surveys in well TR-4. During the warm-up no significant feed zones were observed and it is not possible to locate a transition from conductive to convective temperature in the well.

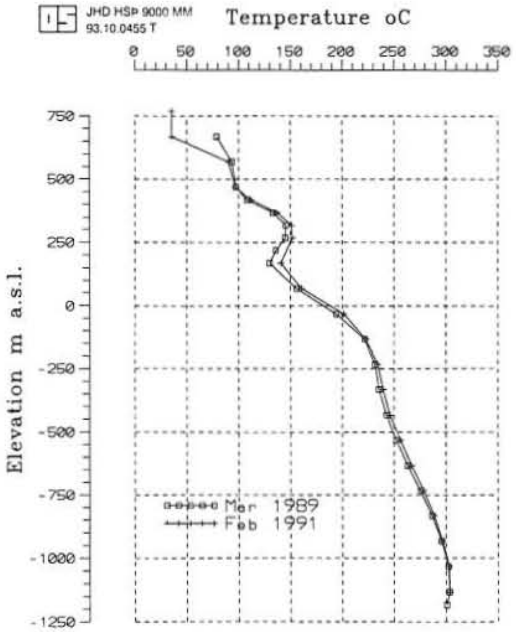

FIGURE 11: Temperature profiles collected in well TR-4

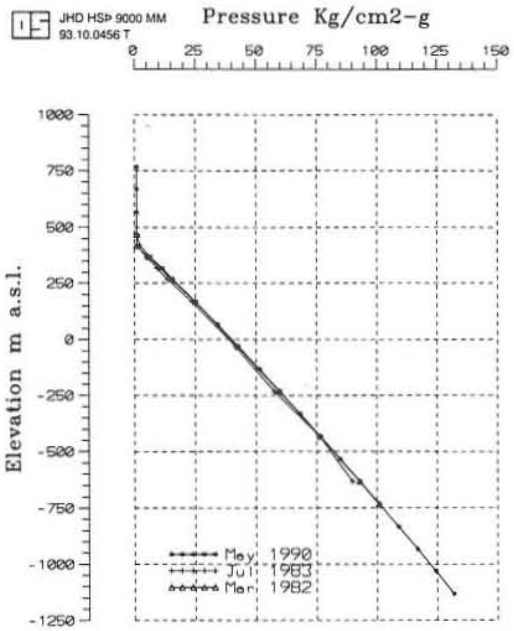

FIGURE 12: Pressure data collected in well TR-4

Similar to well TR-3, a warm aquifer of 150°C is located between +400 to +100 m a.s.l. Another narrow aquifer of intermediate temperature is also intersected from -700 to -850 m a.s.l. A temperature inversion zone is being observed below -1100 m a.s.l. Repeated measurements beneath -1150 m a.s.l. have, however, not been possible due to completion problems.

Negligible changes are observed in the wellbore pressure since 1982 (Figure 12). The pressure at -1000 m a.s.l. is around 122 kg/cm^2-g. This is the highest pressure value reported in the Berlin field at this depth.

Well TR-4 has never discharged continuously, despite several attempts. The well intersected some permeable feedzones (circulation losses 3-5 l/s) during drilling at depths below -1200 m a.s.l. Well TR-4 now serves as a pressure monitoring well for the Berlin field.

Well TR-5: Figures 13 and 14 present several temperature and pressure surveys conducted in well TR-5. During the warm-up period a relatively warm aquifer with temperature higher than 150°C showed up between +300 and +200 m a.s.l.

The main feed zone of the well is believed to be located between -900 to -1100 m a.s.l. No indications of internal flow are seen inside the well. The maximum temperature measured is close to 300°C at -1150 m a.s.l. This well has no sign of reversed temperature beneath the main feedzones likes wells TR-2, TR-3 and TR-4.

The pressure profiles gathered in the well show stable reservoir pressure despite several flow tests conducted in the well. The reservoir pressure at -1000 m a.s.l. is believed to be close to 121 kg/cm^2-g.

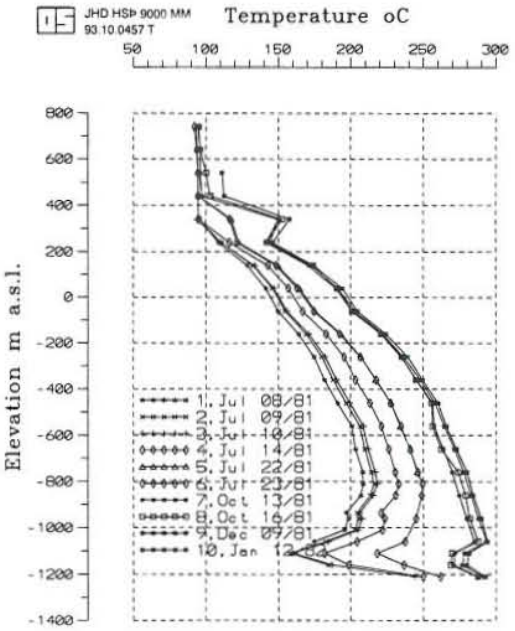

FIGURE 13: Temperature surveys collected during warm-up of well TR-5

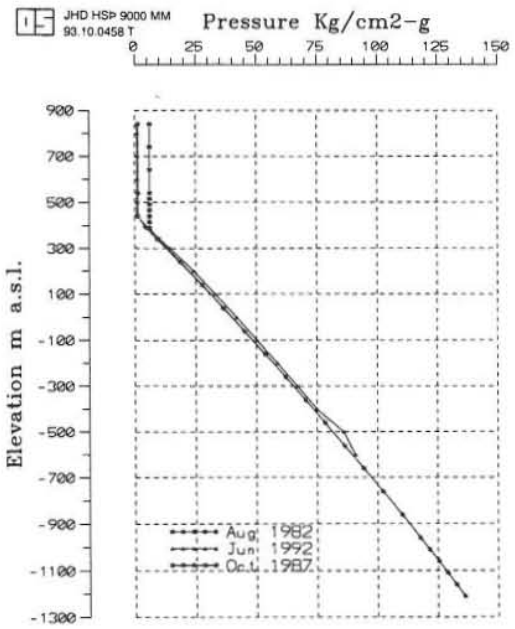

FIGURE 14: Pressure profiles from well TR-5

Well TR-9: Figures 15 and 16 show temperature data from well TR-9 collected during the warm-up period and for several years of shut-in conditions. The main feedzones are located between -900 to -1200 m a.s.l., in addition to a narrow, intermediate aquifer at -400 m a.s.l. The maximum feedzone temperature measured is 290°C at -1000 m a.s.l. An inversion zone is again observed in this well in the bottom part.

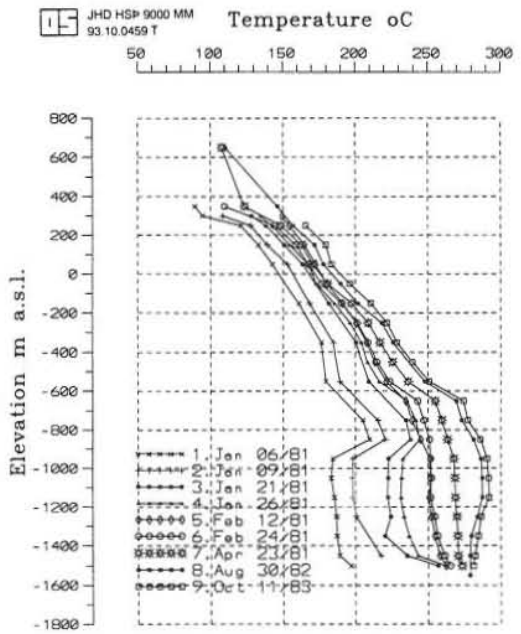

FIGURE 15: Temperature surveys during warm-up of well TR-9

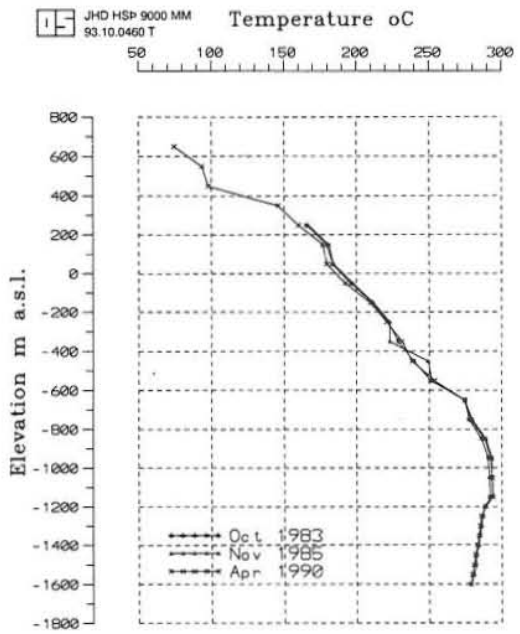

FIGURE 16: Temperature profiles in well TR-9

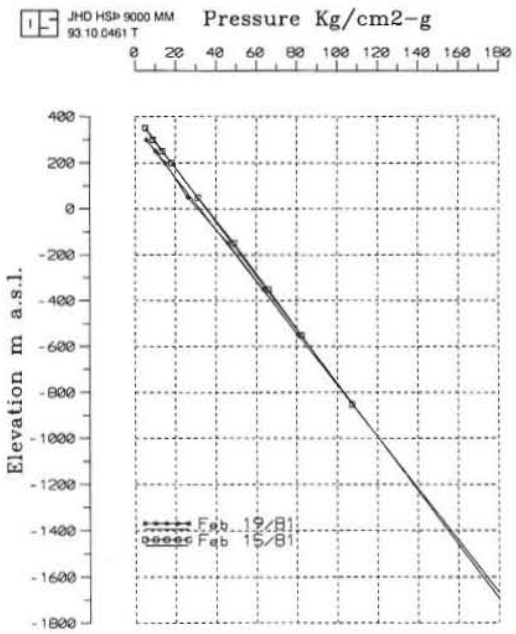

FIGURE 17: The pivot point of well TR-9

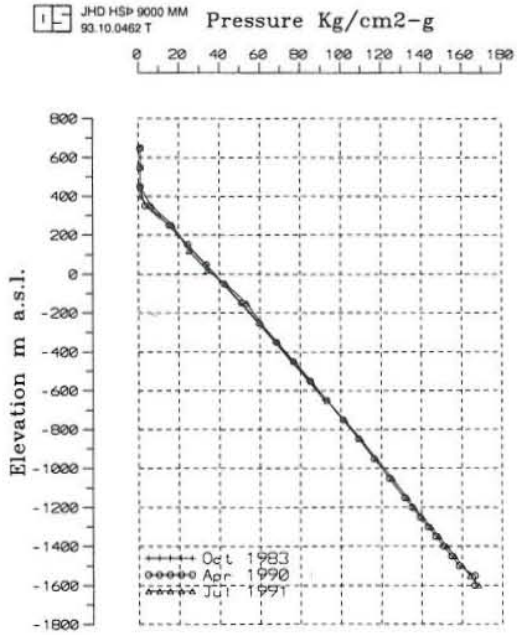

FIGURE 18: Pressure data from well TR-9

Figures 17 and 18 show pressure data from well TR-9. A pivot point analysis shows a stable pressure from -800 to -1200 m a.s.l. with pressure close to 121 kg/cm^2-g at -1000 m a.s.l.

No significant changes have been observed in the downhole conditions of well TR-9 since 1983, despite several discharges. This well was used as a reinjection well from February 1992 to May 1993 and some cooling resulted by the injected fluid.

3.3 Temperature and pressure distribution in the Berlin reservoir

A total of 274 temperature logs and 184 pressure logs were available from the Berlin wells for this study. A standard procedure was used to determine formation pressure and temperature for each of the wells in the data set. Most of the wells have no internal flow during shut-in conditions and the downhole surveys were conducted through several years of no production. Therefore, most of the formation properties were determined simply by plotting temperature and pressure with time at a constant depth. This was especially applicable for the temperature data. The downhole pressure, on the other hand, is usually controlled by only one feedzone in the well. It is, therefore, only representative for the formation pressure at the feedzone elevation. In such cases, the formation temperature profile was used to calculate the downhole pressure curve in a hydrostatic column, which intersected the given feedzone pressure.

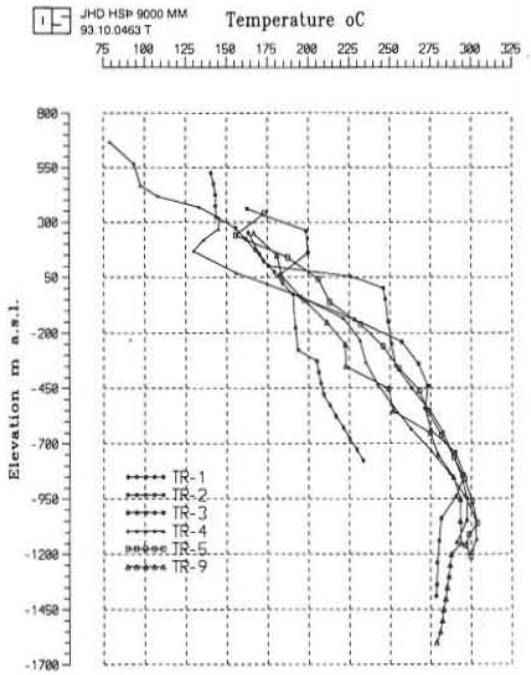

FIGURE 19: Formation temperatures of the Berlin wells

Table 2 summarizes the outcome of the formation pressure and temperature analysis and Figure 19 shows the formation temperature of all wells plotted together.

TABLE 2: Estimated formation temperatures and pressures in the Berlin wells

TR-1			TR-2			TR-3		
Depth (m)	Temp. (°C)	Pressure (bar-a)	Depth (m)	Temp. (°C)	Pressure (bar-a)	Depth (m)	Temp. (°C)	Pressure (bar-a)
160	105	1.01	325	100	1.01	320	102	1.01
400	166	22.6	700	187	34.3	400	163	8.2
500	180	31.4	800	200	42.9	500	199	16.9
600	190	40.0	900	218	51.3	600	200	25.4
700	190	48.7	1000	237	59.5	700	183	34.0
800	191	57.3	1100	252	67.4	800	196	42.6
900	205	65.8	1200	268	75.1	900	228	51.0
1000	208	74.3	1300	275	82.7	1000	258	58.9
1100	214	82.7	1400	281	90.1	1100	268	66.6
1200	220	91.0	1500	290	97.4	1200	273	74.2
1300	230	99.3	1600	293	104.6	1300	271	81.7
1400	236	107.5	1700	297	111.8	1400	275	89.2
1500	245	115.5	1800	297	118.9	1500	290	96.6
			1900	295	126.1	1600	295	103.8
						1700	291	110.9
						1800	281	118.3
						1900	280	125.7
						2000	279	133.2
						2100	279	140.7

TR-4			TR-5			TR-9		
Depth (m)	Temp. (°C)	Pressure (bar-a)	Depth (m)	Temp. (°C)	Pressure (bar-a)	Depth (m)	Temp. (°C)	Pressure (bar-a)
350	100	1.01	350	100	1.01	240	100	1.01
500	145	14.4	600	156	24.2	500	181	23.7
600	130	23.6	700	188	33.0	600	184	32.4
700	156	32.6	800	206	41.5	700	198	41.0
800	194	41.4	900	213	49.9	800	212	49.5
900	222	49.8	1000	232	58.2	900	223	57.8
1000	232	58.0	1100	246	66.2	1000	223	66.1
1100	235	66.1	1200	256	74.1	1100	249	74.1
1200	243	74.1	1300	268	81.8	1200	252	82.0
1300	252	82.1	1400	274	89.3	1300	275	89.7
1400	263	89.8	1500	281	96.8	1400	280	97.1
1500	275	97.4	1600	289	104.1	1500	289	104.5
1600	287	104.8	1700	296	111.3	1600	293	111.7
1700	296	112.1	1800	300	118.4	1700	293	118.9
1800	302	119.1	1900	304	125.4	1800	294	126.1
1900	303	126.2	2000	297	132.5	1900	287	133.4
						2000	285	140.8
						2100	283	148.2
						2200	281	155.7

Figures 20 and 21 show temperature and pressure contours at -1000 m a.s.l., based on the data in Table 2. The temperature and the pressure contours were made in a 3x3 km mesh and cover the actual geothermal field and its surroundings in N-S coordinates from 265,000 to 268,000 m and E-W coordinates from 551,000 to 554,000 m.

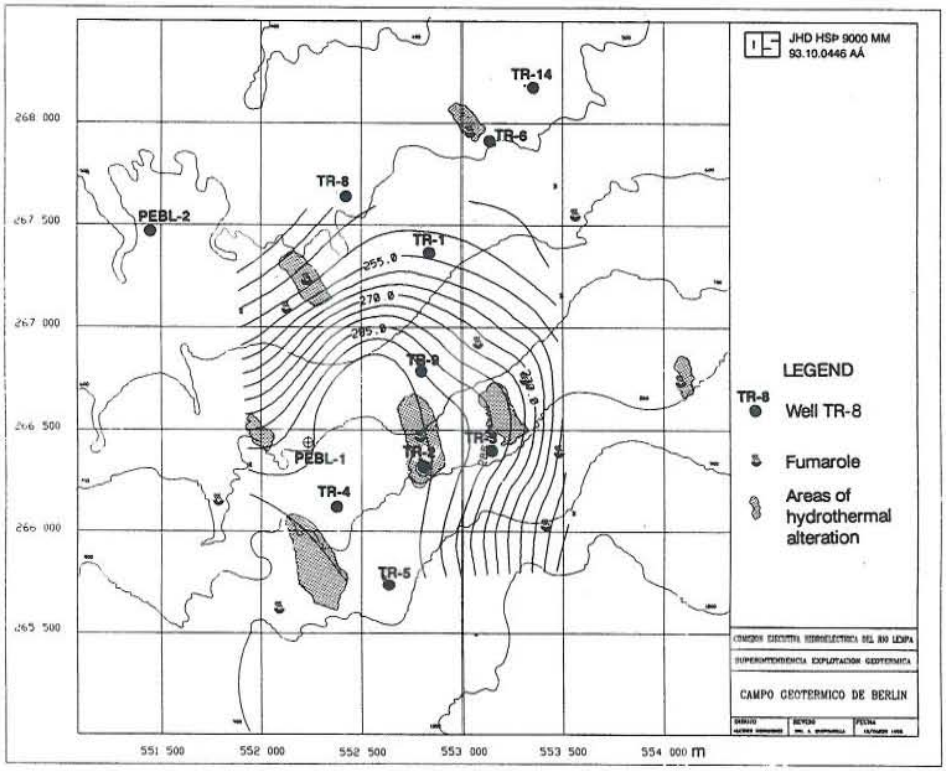

FIGURE 20: Temperature contours at -1000 m a.s.l. in the Berlin geothermal field

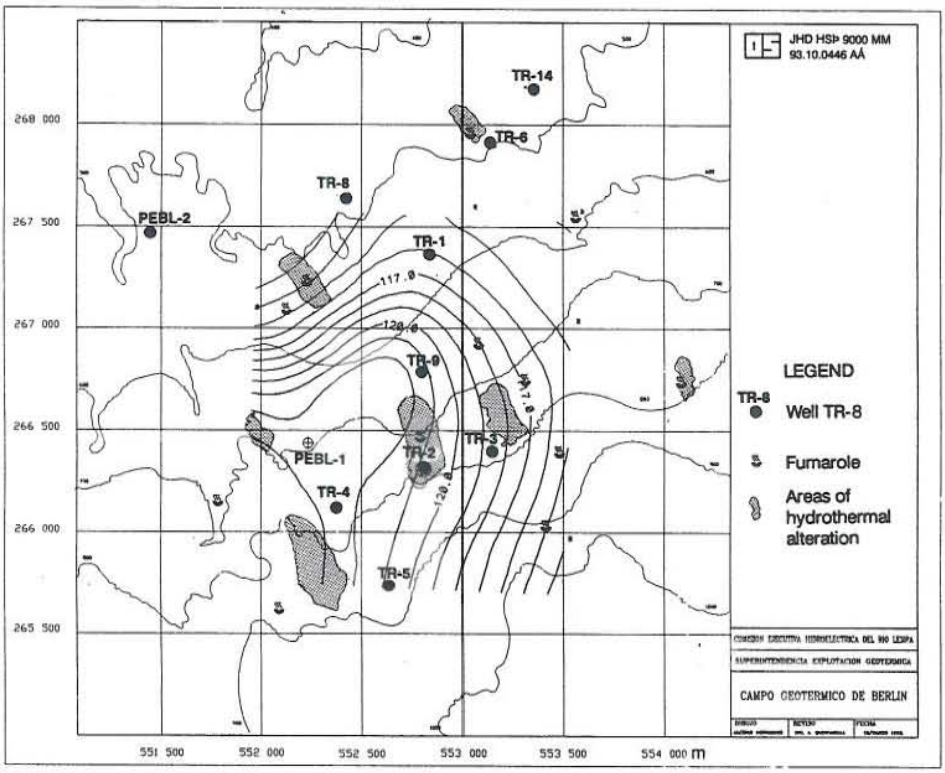

FIGURE 21: Pressure contours at -1000 m a.s.l. in the Berlin geothermal field

The contour plots identify an upflow zone located to the south and southwest from the present wellfield, and a horizontal flow path away from it is directed northnortheast just inside the caldera rim. This flow makes a change in direction in the eastern part of the wellfield, where it changes to a northnorthwesterly direction. A similar flow path is seen in the pressure contours.

Figures 22 and 23 show two temperature cross sections directed N-S and E-W. These were drawn in order to analyze temperature variations with depth in the deep Berlin wells. Both figures show a horizontal fluid flow at -900 to -1200 m a.s.l., initially towards northeast and later on to a northnorthwesterly direction. This is in good correlation with the faulting in this region (Figure 1).

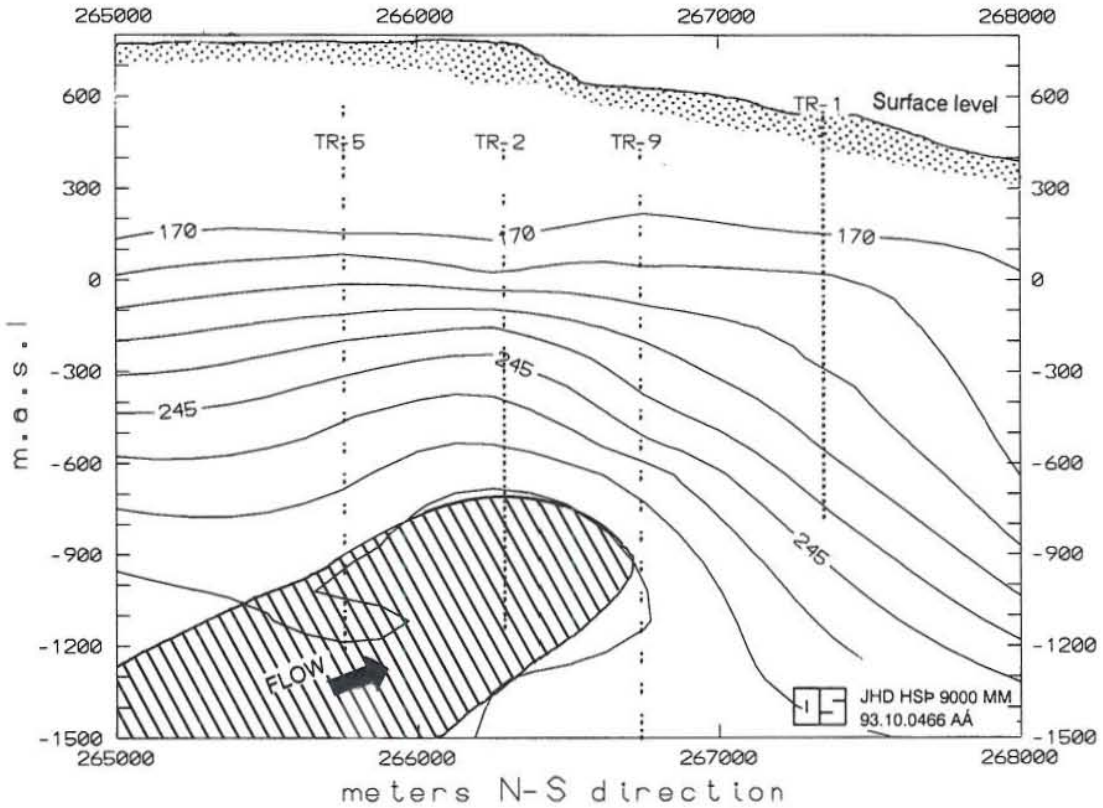

FIGURE 22: A N-S temperature cross section through wells TR-1, TR-2, TR-5 and TR-9

It should be noted that some linear extrapolation was used to determine the location of temperature and pressure contours outside the Berlin wellfield and caldera. Figures 20-23 should therefore be taken as the author's interpretation, which may change as more wells are drilled.

3.4 Production data

The productive Berlin wells have all undertaken flow tests lasting from several days up to years. These flow tests indicate very good production characteristics and the wells provide up to 90 kg/s of 1300 kJ/kg fluid. Wells TR-2, TR-5 and TR-9 must be air compressed to 30 bars in order to stimulate discharge. Well TR-3, on the other hand, maintains a wellhead pressure of 3 bar-a, which is enough for initiating discharge.

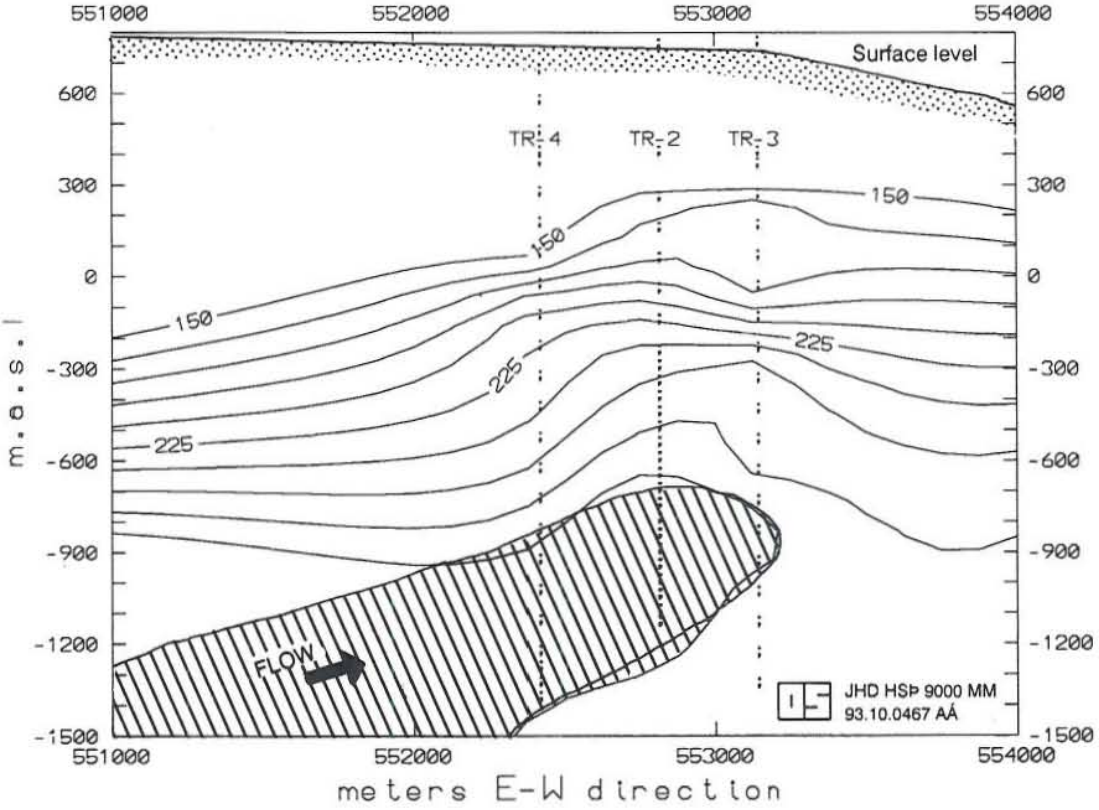

FIGURE 23: An E-W temperature cross section through wells TR-2, TR-3 and TR-4

Well TR-1 is the least producer at present. Its discharge at 4 bar-a wellhead pressure is between 10 and 15 kg/s with enthalpy between 800 to 1200 kJ/kg. Due to this low productivity, well TR-1 is being used as a reinjection well.

As stated earlier, well TR-4 has not discharged yet, despite promising thermodynamic characteristics at its deeper part. This has to do with a drill string and fishing tools, left in the well.

Table 3 summarizes the main production characteristics of wells TR-2, TR-3, TR-5 and TR-9 at 10 bar-a wellhead pressure. Figures 24 to 27 show the output curves for these wells.

TABLE 3: Production data for some Berlin wells at 10 bar-a wellhead pressure

Well	Total flow (kg/s)	Steam flow (kg/s)	Dryness (%)	Enthalpy (kJ/kg)	Shut-in pressure	PI (10^{-11}m^3)
TR-2	87	26	30	1350	33 bar-a	> 1
TR-3	38	10	27	1280	20 bar-a	0.9 - 1.0
TR-5	62	19	31	1370	38 bar-a	0.5
TR-9	36	10	28	1300	19 bar-a	0.9 - 1.0

PI: Productivity Index

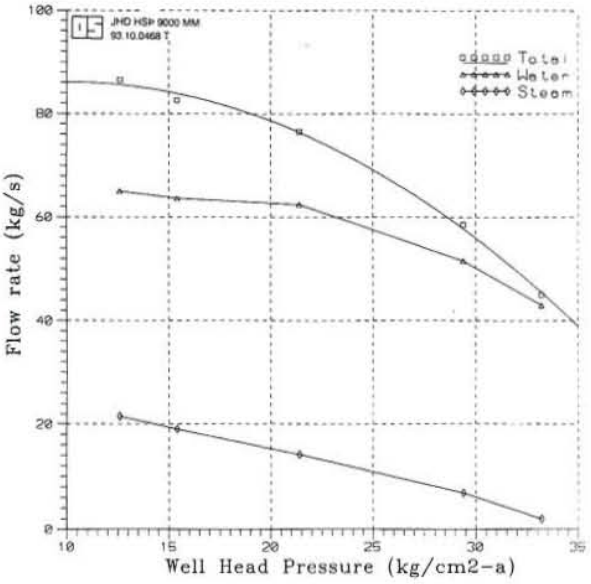

FIGURE 24: Output curve for well TR-2

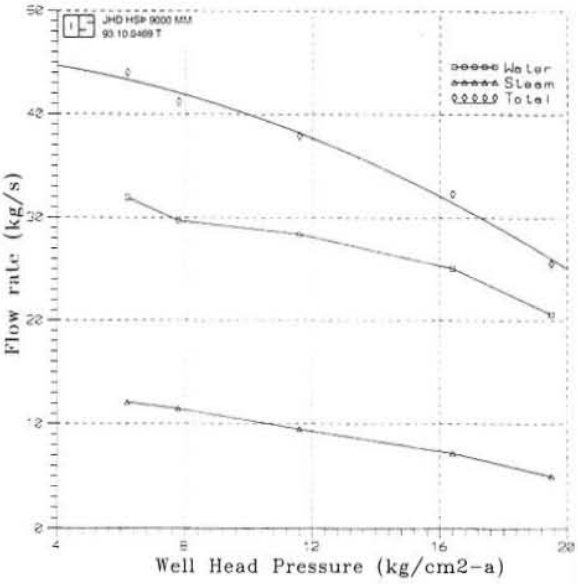

FIGURE 25: Output curve for well TR-3

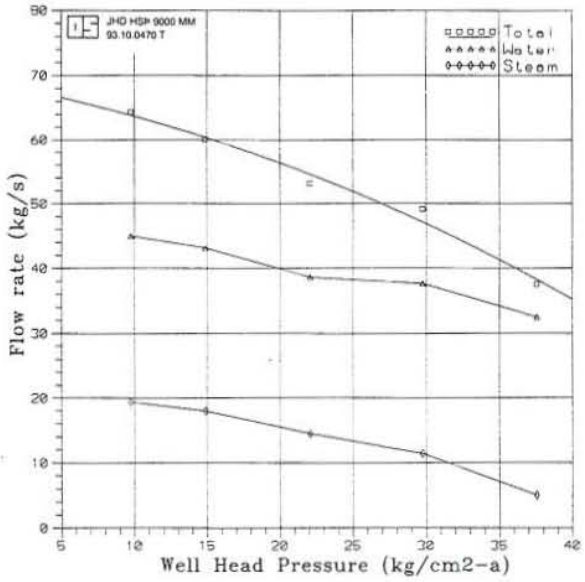

FIGURE 26: Output curve for well TR-5

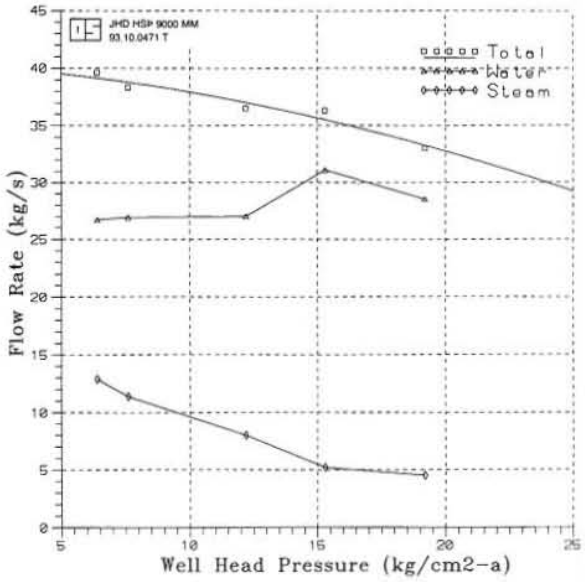

FIGURE 27: Output curve for well TR-9

The last column of Table 3 contains a productivity index (PI) for the four wells. This index was evaluated by using the multi-feedzone wellbore simulator HOLA (Bjornsson and Bodvarsson, 1987). The procedure was as follows. For each well, the programme HOLA was used to calculate the output curve for a given productivity index and varying bottomhole pressure. This calculated output curve was compared with the real one and index changes made until a satisfactory match was obtained. Unfortunately, no flowing pressure and temperature profiles were available from the Berlin wells to constrain this kind of a study.

The wellbore simulation study indicates that wells TR-2, TR-3, TR-5 and TR-9 all flash down to their bottom during discharge and even some distance into the reservoir. A comparison between the enthalpy data in Table 3 and the formation temperature at the permeable zone at -1000 m a.s.l. (Table 2), shows that the flowing enthalpy is slightly higher than the enthalpy of the static reservoir fluid. Therefore, flashing all the way into the formation during discharge is quite

possible. This also leads to the important conclusion that increased enthalpy of production wells is to be expected in the future as the reservoir pressure declines and the two-phase reservoir zone becomes extended.

3.5 Interference data

During February 1992 until May 1993, a large scale production testing was carried out in the Berlin field. Around 80 kg/s were produced from well TR-2, the fluid separated at 9.0 bar-a and 19 kg/s of steam piped to one of the two back pressure units installed. The separated fluid, on the other hand, was reinjected into wells TR-1 and TR-9 at 15 and 42 kg/s flowrate, respectively. In July 1992, after six months of continuous production, the fluid extraction was stopped due to mechanical problems in one of the turbines. The power generation was restarted on October 31 1992 by using the other unit, and went on until May 1993 when the production test was stopped.

Table 4 summarizes the production data collected during the test.

TABLE 4: Flowrates during a production test in the Berlin field

Well	Period	Days	Flow rate (kg/s)	Mass Ext/Inj (kTons)	WHP (bar-g)
TR-2	Feb 4 - Jul 11	157	79.1	1073	11.2
	Jul 11 - Oct 5	86	0	0	0
	Oct 5 - Feb 5/ 93	123	86.2	916	11.4
	Feb 5 - May 31	117	86.2	871.4	11.4
TR-9	Feb 4 - Jul 11	157	-42.4	-575.1	6.2
	Jul 11 - Oct 5	86	0	0	-
	Oct 5 - Feb 5/ 93	123	-49.1	-521.8	5.8
	Feb 5 - May 31	117	-53.4	-540	5.8
TR-1	Feb 4 - Jul 11	157	-14.3	-194	8.5
	Jul 11 - Oct 5	86	0	0	-
	Oct 5 - Feb 5/ 93	123	-9.7	-104	7.8
	Feb 5 - May 31	117	-6.5	-65.5	7.8

Note: Negative flowrates indicate injection

As a part of this production test, a capillary tubing system was installed in well TR-4 and connected to a Sperry Sun data logger. The suspension chamber at the end part of the capillary tube is located at sea level. Figure 28 shows the pressure response of well TR-4 due to the production from TR-2 and reinjection into TR-1 and TR-9. As is seen in the figure, a clear pressure interference occurred over the 435 m horizontal distance between wells TR-2 and TR-4. A total pressure drawdown of only 0.5 bars was observed, which is well above the scatter seen in the collected data.

The computer programme VARFLOW was used to analyze the interference data in order to evaluate the main reservoir properties. The VARFLOW code calculates pressure changes in a horizontal, single phase, isothermal and confined reservoir due to fluid production/injection (Lawrence Berkeley Laboratory, 1982). In this study only an isotropic, infinite reservoir was considered due to the limited information available on the reservoir structure. Several simulations were made. Figure 28 shows results for three cases of different reservoir properties. A "best" matching was obtained for the two values of transmissivity (T) and storativity (S):

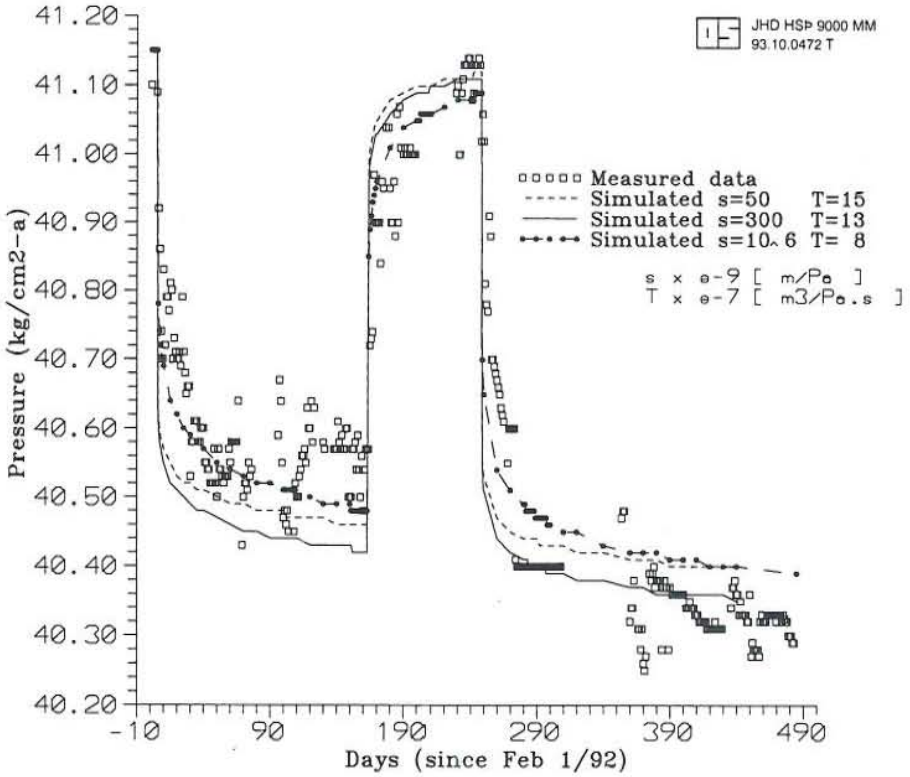

FIGURE 28: Observed and calculated pressure data collected in well TR-4 during an interference test

$$T = \frac{kh}{\mu} = 13\times10^{-7}\ \frac{m^3}{Pa}$$

and

$$S = \phi c_t h = 300\times10^{-9}\ \frac{m}{Pa}$$

where k is the reservoir intrinsic permeability, h is its thickness, μ is the fluid dynamic viscosity, ϕ is the reservoir porosity, c_t is the total reservoir compressibility, taken as $c_t = \phi c_w + (1-\phi)c_r$ where c_w and c_r are the water and rock compressibilities respectively.

Assuming 300°C reservoir temperature and 10% porosity gives the permeability thickness

$$kh = 117\ mD$$

and the product of the reservoir porosity and thickness

$$\phi h = \frac{300\times10^{-9}}{1\times10^{-9}} = 300\ m$$

The above values indicate a 2-3 km thick reservoir of 40-60 mD permeability. These should be compared with the 20-30 mD evaluated for the Ahuachapan reservoir in a recent simulation study (Lawrence Berkeley Laboratory, 1991). However, part of the high storativity may be due to boiling in the reservoir. This will reduce the reservoir thickness from the values shown above and, hence, increase the intrinsic permeability.

4. A CONCEPTUAL RESERVOIR MODEL

In the previous chapters, a brief summary is given on the geological and geophysical studies conducted in the Berlin field, the formation pressures and temperatures were evaluated and production characteristics of the wells and the wellfield discussed. In Figure 29, an attempt is made to unify the results of these studies into a single conceptual model for the Berlin geothermal system. The main parts of the model are as follows:

1. Upflow zone of ≥300°C liquid water at the inner part of the Berlin caldera. This is based on the temperature distribution, geology and high ratios of CO_2/H_2S gases and gas/steam ratios in fumaroles above the proposed upflow zone.

2. Lateral flow at -1000 m a.s.l. towards northeast, probably due to the combined influence of northeast trending faults in this area and horizontally permeable layers. This conclusion is strongly supported by a temperature reversal in the lower part of the deep Berlin wells.

3. Change in flow direction towards northnorthwest at the eastern part of the wellfield. This is due to young and active faults of the same direction in this area. The fluids migrate up to the surface and are seen as fumaroles and hot springs at Santa Anita river basin. The low resistivity tongue towards northnorthwest delineates this outflow zone (Figure 1).

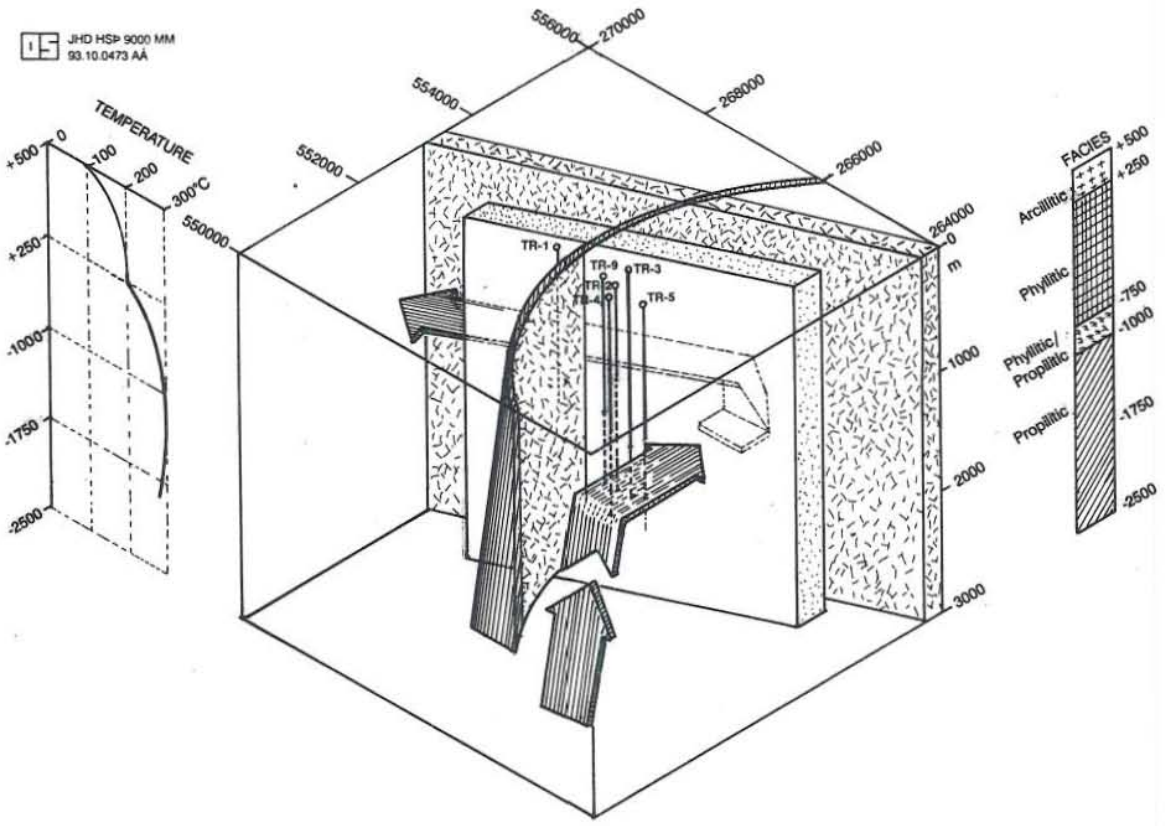

FIGURE 29: A conceptual reservoir model of the Berlin geothermal system; the arrows denote the main flow paths of the geothermal fluid

4. The inner caldera rim, as observed on the surface, is taken to be a flow barrier, except where it is intersected by the young northnorthwesterly trending faults. This assumption has weak support through the low permeability of well TR-1, which is the only deep well drilled out of the caldera rim, and by the fact that the majority of fumaroles in the Berlin area are located within the caldera.

5. Another, low permeable structure is taken to be to the east of the wellfield, and is supported by high resistivity in this region (Figure 1).

6. The formation temperature of wells indicates two reservoirs of horizontal flow, a shallow one at sea level of low salinity and temperature around 200°C, and a deeper one at -1000 m a.s.l. This is the main production zone of the Berlin field. The deep reservoir temperature is between 270 and 300°C and the fluid has rather high salinity. A weak support is for a third narrow aquifer at -500 to -700 m a.s.l.

7. A comparison of the pressure and the temperature data indicates that all of the three reservoirs are in liquid state except for the upper part of the shallow aquifer, which may have a free surface and boiling curve with depth some tens of meters down. Most of the pressure data is influenced by the deep reservoir only, as pivot points of wells are mainly located there. A comparison of pressure data in well TR-1, which is controlled by the shallow reservoir, and pressure data in other wells, indicates hydrostatic equilibrium between the shallow and the deep reservoir.

8. The deep reservoir seems to be of high permeability, probably between 50 and 100 mD. This permeability may be secondary and due to tectonic faulting and fracturing.

5. NUMERICAL 3-D MODELLING

5.1 Modelling approach

One part of the 1993 UNU reservoir engineering programme consisted of operating the geothermal simulator TOUGH. The acronym TOUGH stands for "Transport Of Unsaturated Groundwater and Heat" and is a multi-dimensional numerical model for simulating the coupled transport of water, vapour, air and heat in porous and fractured media. It is a member of the MULKOM family of multi-phase, multi-component codes, which are being developed at the Lawrence Berkeley Laboratory in California (Pruess, 1987).

The numerical approach is based on the integral difference method, which permits simulation of one, two or three dimensional systems. This formulation easily handles both regular and irregular grid block geometries. The differential equations are formulated fully implicitly and all mass and energy balance equations are solved simultaneously by using the Newton-Raphson iteration and a direct solution technique.

In this study, the TOUGH simulator was used to simulate the Berlin reservoir. The basic approach is the same as given by Bodvarsson et al., (1986). It first deals with the development of a conceptual reservoir model that must be consistent with all the data collected in the field. When a reasonable conceptual model has been developed, it should initially be tested against the natural thermodynamic conditions of the field, i.e. undisturbed condition of the field prior to exploitation. This "natural state" model is developed using trial and error procedures until it matches the spatial distribution of temperatures and pressures. When fully developed, the natural state model will allow the determination of the rate of fluid and heat recharge and discharge, the flow of mass and heat within the system, and yield a coarse estimate of the permeability distribution.

Once a natural state model has been developed, it must be calibrated against pressure tests (especially long-term interference tests), and production history. The adjustments needed to match the production history, often require recalibration of the model in natural state. This procedure of calibrating the natural state and the production reservoir model is continued until a good matching has been obtained for all the available data, providing finally one and the same reservoir model for both the natural state and the production testing.

After a "best" reservoir model has been developed, which is consistent with all the data considered, it is generally advisable to conduct some sensitivity studies, especially regarding the most important parameters that affect the performance predictions. Usually, these parameters are the permeability and the porosity distribution and the assumed nature of the reservoir boundaries (e.g. closed reservoir, infinitive acting reservoir, constant pressure boundaries). The pressure decline is primarily controlled by the permeability distribution and the outer boundary conditions, whereas the enthalpy changes are primarily controlled by the porosity and the temperature distribution. After the sensitivity studies are completed, a conservative model should be chosen and used for performance predictions.

The following text presents a coarse, numerical simulation of the natural state data and the production data from the Berlin field. Due to the limited time and data available for the study, no performance predictions were made.

5.2 The numerical grid

Figure 30 shows an area view of the numerical grid that was developed for the Berlin field.

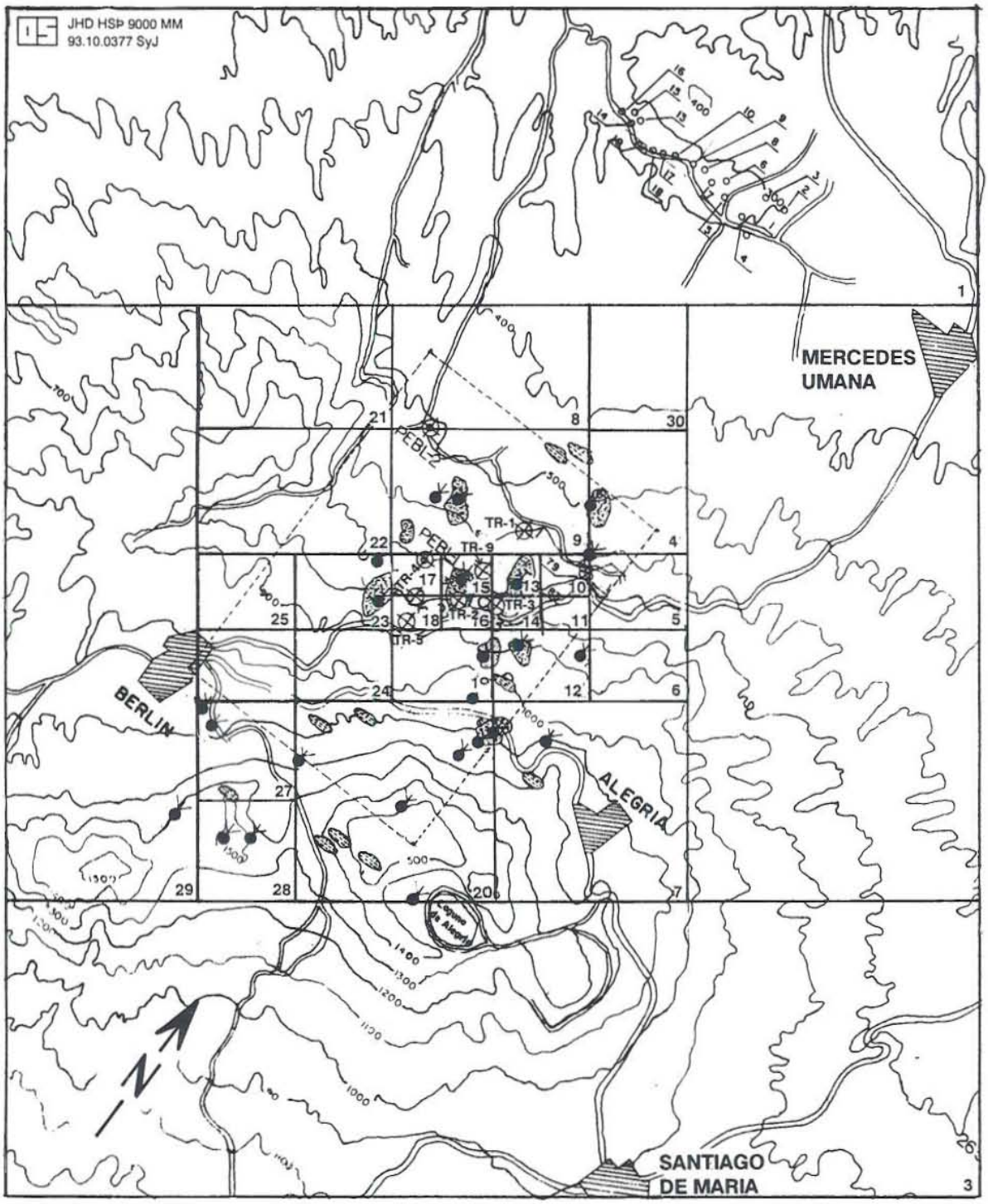

FIGURE 30: The numerical grid used for modelling the Berlin field

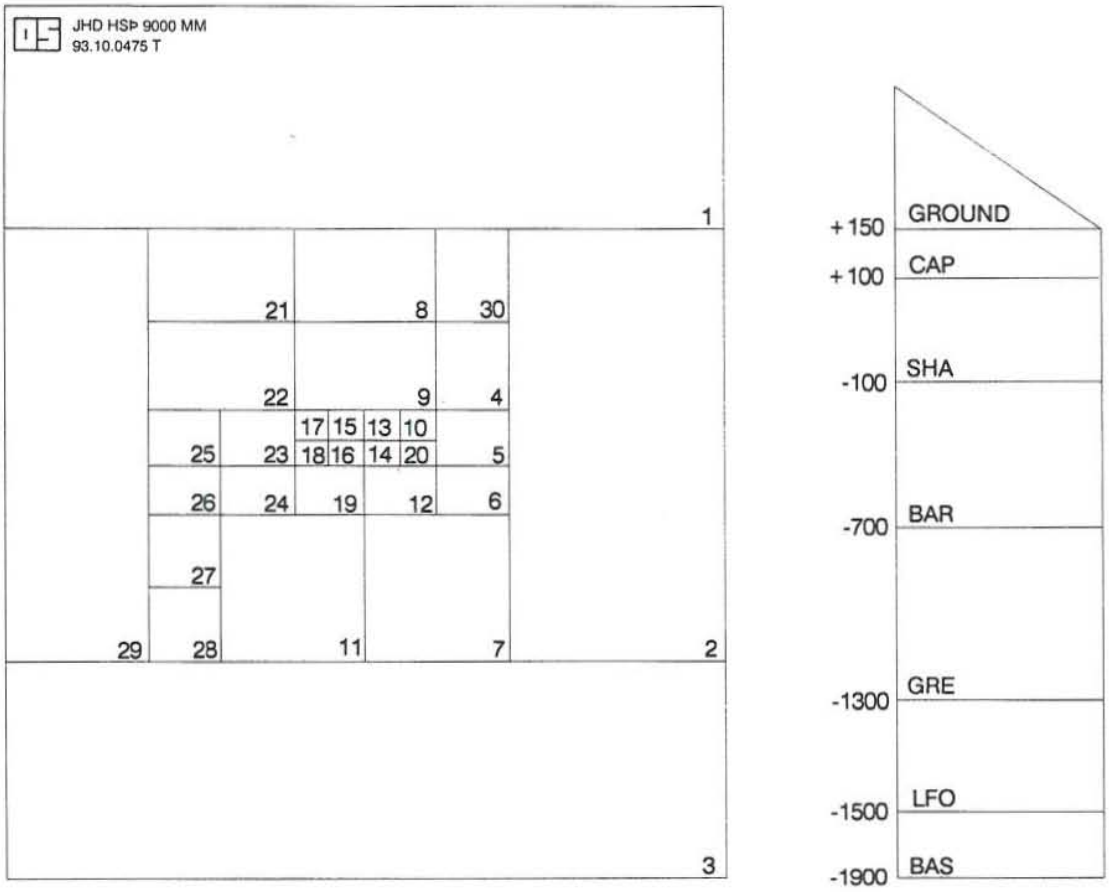

FIGURE 31: Distribution of layers in the Berlin numerical grid

Figure 31 shows the layering of the grid. The side lengths are 10x12 km. Each grid layer was divided into 30, irregularly sized blocks. The total number of blocks is 152 and they are interconnected by 530 connections. For simplicity, only rectangular grid blocks were considered.

The numerical grid consists of 5 layers which all have the same grid geometry (Figure 31). They are as follows:

a) A **caprock** layer, which is a low permeability zone
b) A **shallow aquifer,** representing the shallow reservoir
c) A **barrier,** which is separating the shallow and the deep Berlin reservoirs
d) The **geothermal reservoir,** which represents the productive reservoir
e) A **lateral flow** layer, used to induce temperature reversal in the lower part of the system.

The vertical peripheries of the above 5 layers are kept impermeable, both for heat and mass flow. A single block **Basement** layer is introduced underneath the lateral flow layer. This layer has a negligible permeability and constant temperature. Similarly, a single **Groundwater** block is placed on the top of the caprock. These layers serve as constant pressure and temperature boundaries, simulated by very high block volumes and heat capacities. The groundwater block has connections to all the caprock blocks. However, the length of the connection increases with increased elevation, in order to simulate the steep slopes of the Berlin mountain (assuming a rise in the groundwater level with elevation). One of the presumptions made in the modelling work, was to minimize the number of rock properties used for the matching. Table 5 presents these properties.

In general, low permeability and porosity were assigned to the boundary blocks, whereas high values are used in the centre of the 5 horizontal grid layers. The grid density was constructed in the same way, i.e. high density at the centre, representing the well known wellfield, and coarse at the unknown boundaries. Figure 32 shows how the different rock properties were assigned to the 5 layers of the numerical grid. Table 6 shows finally the block numbers that present the deeper wells in the Berlin field.

TABLE 5: Rock properties used in the numerical simulation

Rocks	Permeability (mD)	ϕ (%)	Layer	Description
CAPRK	0.1-0.01	5	Caprock, Barrier, Shallow reservoir	Superficial layer that isolates the system from the overlaying groundwater, lateral boundaries and intermediate barrier
SHAQU	5-10	5	Shallow	Shallow thermal aquifer located close to sea level
WELLF	25-100	10	Reservoir	Productive geothermal reservoir
DISCH	1-5	10	Barrier	Areas where thermal fluids go up, used to simulate hot spring areas, and flow between the deeper and the shallow reservoir
SURFA	1-10 (10^3)	20	Groundw	Used to simulate the regional groundwater system
BASEM	0.00001	5	Basement	Impermeable basement of the system

The range shown in permeability reflects the sensitivity of the parameter.

TABLE 6: Grid block numbers for the Berlin wells

Well name	Block number
TR-1	9
TR-2	16
TR-3	14
TR-4	17
TR-5	18
TR-9	

5.3 Natural state simulations

The initial conditions to be used in the natural state modelling were estimated by considering the system in a thermal equilibrium, that is without convective flow. An average thermal conductive gradient of 0.12 to 0.15°C/m was used to define the initial temperature, uniform for the individual layers. The pressure, on the other hand, was calculated as a hydrostatic water column of density 1000 kg/m^3.

Table 7 shows the numerical values used for the initial conditions of the natural state model.

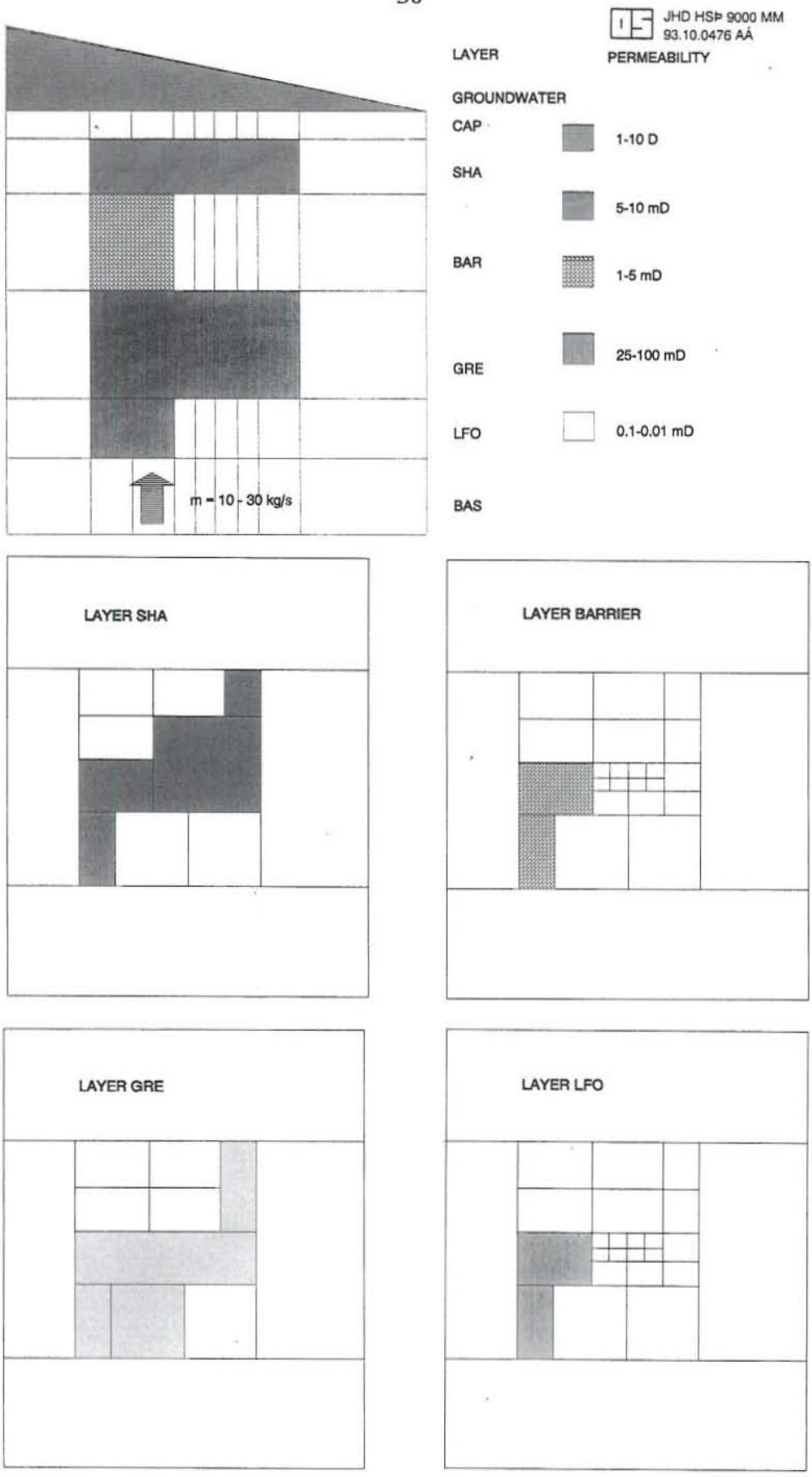

FIGURE 32: Distribution of reservoir properties in the 3-D grid

TABLE 7: Initial conditions for natural state simulations of the Berlin reservoir.

Layer	Ref.depth (m a.s.l.)	Pressure (bar-a)	Temperature (°C)
Surface	+125	1.0	55
Caprock	+125	12.0	75
Shallow	0	40.0	120
Barrier	-400	68.0	160
Reservoir	-1000	119.0	260
Lateral flow	- 1400	153.0	275
Basement	-1700	178.0	290

The simulation work mainly consisted of balancing the inflow to the system, the permeability of the caprock and the length of the connections to the groundwater layer. The source was placed at block LFO 28 in the lateral flow layer (Figure 31). By using trial-and-error procedure, a final inflow rate of 30 kg/s and 1400 kJ/kg enthalpy resulted.

The steady inflow of 30 kg/s of 1400 kJ/kg fluid was maintained for 100,000 years. Figure 33 shows the temperature and pressure history of block GRE16 in the centre of the wellfield during this stage. The figure shows clearly that the model is in stable condition after this period of time. Figure 34 shows a comparison between the measured wellbore temperature and the calculated

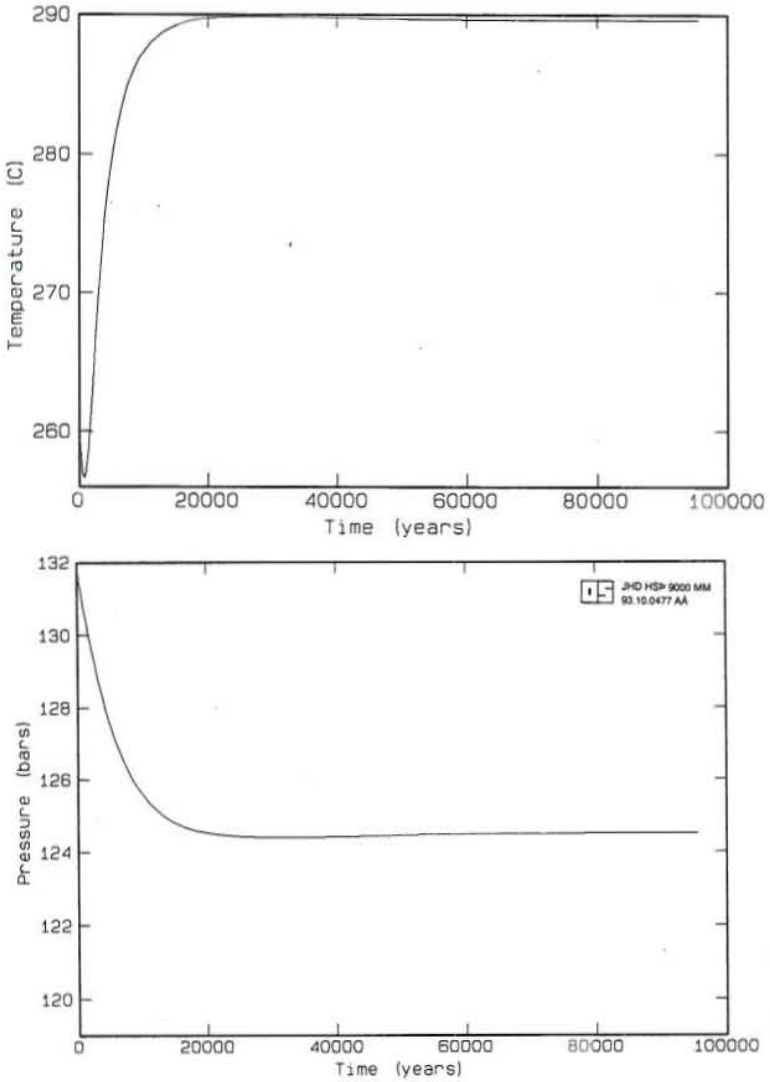

FIGURE 33: a) Temperature and b) pressure of block GRE16 during 100,000 years of warm-up

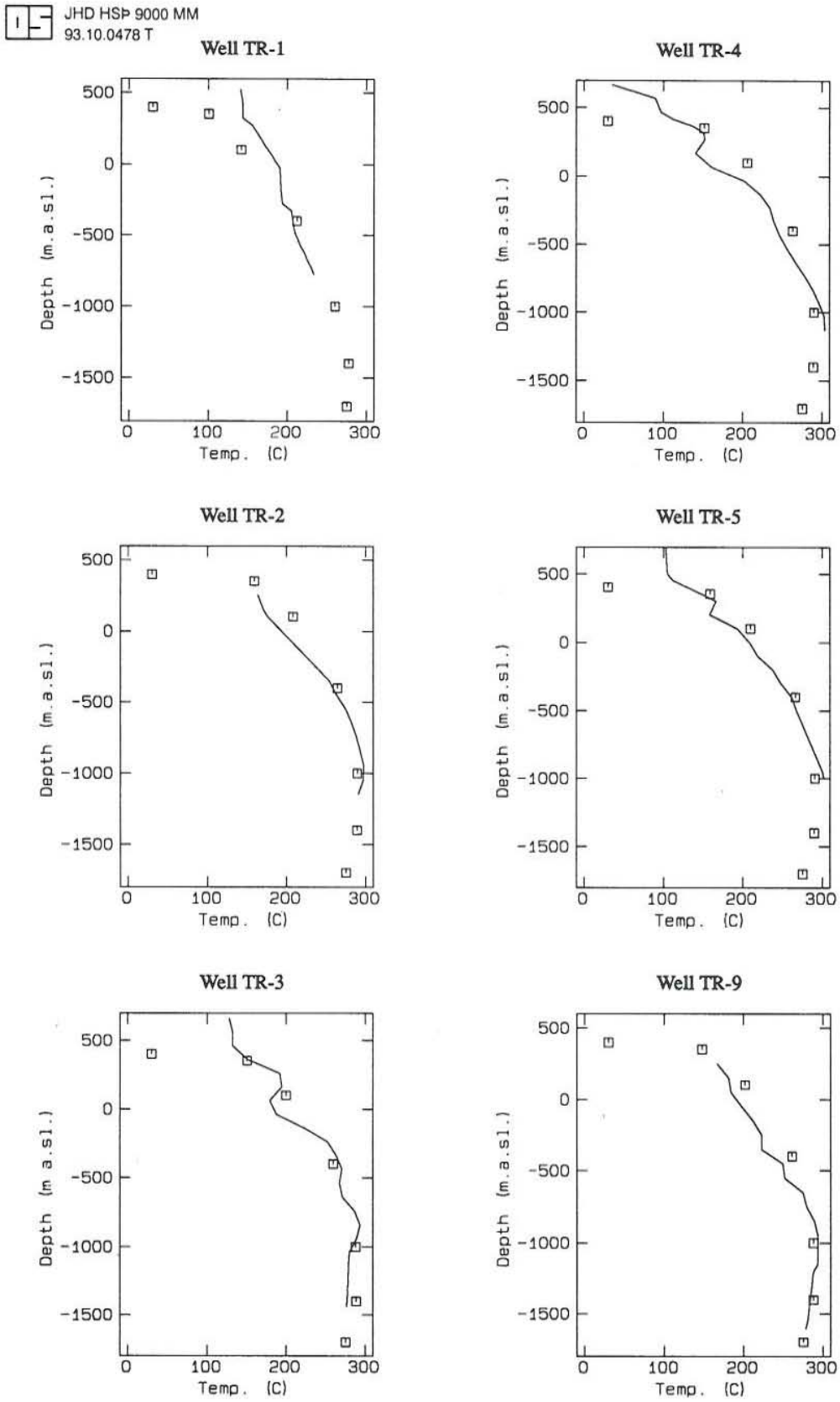

FIGURE 34: Simulated and measured temperatures in the Berlin wells

temperature profiles in the 3-D grid and Figure 35 shows finally the difference between the measured and the simulated pressure.

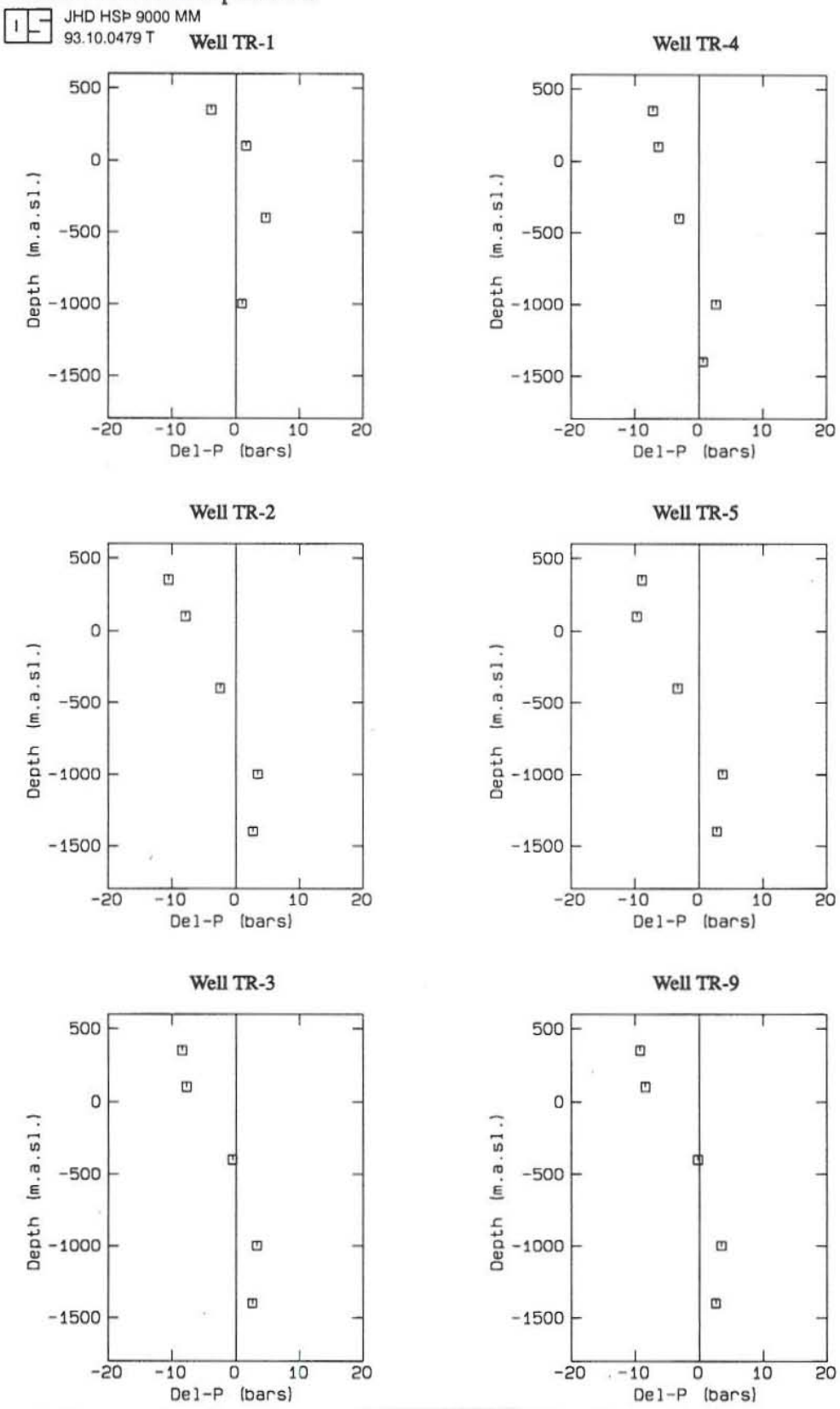

FIGURE 35: The difference between simulated and measured pressure in the Berlin wells

A simple sensitivity study was carried out in order to check the influence of some selected reservoir parameters on the total performance of the model. The permeability was found to be the most important parameter, but could for most layers be changed within a maximum of one order of magnitude. As an example, changes in the permeability of the deep reservoir (GRE) from 20 to 120 mD had minor effects on the pressure and temperature distribution in the model. The caprock and some discharge blocks, on the other hand, showed to be very sensitive to the model performance. As an example, fluctuating flow direction in the caprock, showed up if the caprock permeability was changed by more than 30% from the matching value. The recharge rate was also found to be very sensitive and had a strong coupling effect with the permeability of the caprock layer.

5.4 Simulating the production data

The second stage in the reservoir modelling of the Berlin field is concerned with simulating the production data from the interference test conducted in 1992-1993 (Figure 28). The production rates, given in Table 3 were specified to the numerical model and pressure changes due to the production calculated. As was expected before hand, some changes had to be done in the model parameters, which again resulted in recalibration of the natural state simulation.

The VARFLOW analysis in Chapter 3.5 showed high storativity in the reservoir. This may have a combination of two explanations, fluid expansion due to boiling or a large volume of the liquid dominated reservoir. Due to limited time available for this study, only the large reservoir volume case was considered here. This was simulated by increasing the volume of the recharge block (LFO 28), from 0.2 km^3 to 60 km^3. Figure 36 shows the match between the measured and the calculated data.

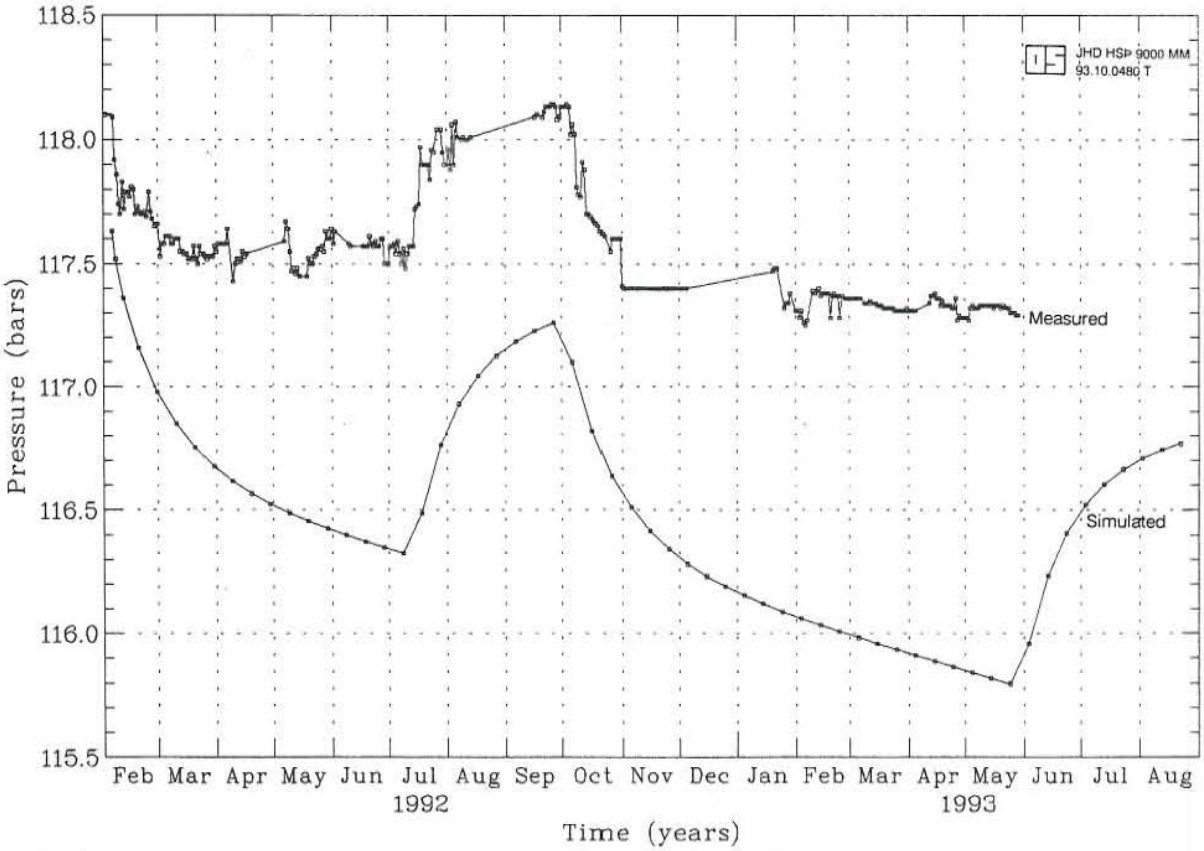

FIGURE 36: Measured and calculated pressure in well TR-4 during an interference test

6. GENERAL RESERVOIR ASSESSMENT FOR THE BERLIN FIELD

It is very important, during the initial stage of a geothermal field development, to estimate the thermal energy available. In this chapter an attempt is made to evaluate the power potential of the Berlin field by using three models for reservoir assessment.

A reservoir assessment refers to a procedure where coarse quantitative estimates are obtained for a large resource. One way of doing this is by a general volumetric assessment. The analysis considers the stored heat of the reservoir for estimating the reserve of available energy. Another option shown here is by a lumped simulation, which is applicable when some production data are available. Finally, additional volumetric computations are made by considering a random distribution in some of the reservoir properties (the Monte Carlo method).

6.1 Volumetric analysis

The volumetric method estimates the "stored heat" contained in the subsurface fluids and rocks, assuming a homogeneous and closed reservoir (no cold or warm recharge). It is considered to be a rather limited but inexpensive method for roughly estimating the power potential of a geothermal reservoir.

The governing equation for the calculations is

$$E_s = E_r + E_f = V\rho_r C_r (1-\phi)(T-T_r) + (V\rho_f \phi\,(h_T - h_r))$$

where

$E_{s,r,f}$	- stored heat in the system, rock, and fluid respectively		
V	- reservoir volume	T	- temperature
h	- enthalpy	C	- rock heat capacity
ϕ	- rock porosity	ρ	- density
r	- rock	f	- fluid
r	- reference temp.	T	- reservoir temperature

The stored heat calculated by the above equation must be converted into useful thermal energy by applying an empirical factor, the so-called *Recovery Factor*. This factor generally ranges up to 25% of the stored heat under general conditions of porosity and permeability. However, in some natural systems it is substantially lower, approaching zero for unfractured and impermeable rocks.

Several papers are available in the geothermal literature discussing the evaluation of recovery factors for various idealized reservoirs (Bodvarsson, 1974; Nathenson, 1975; Nathenson and Mufler, 1975; Banwell, 1963; Mufler and Cataldi, 1977). In some of them, a distinction is made between areas of known and unknown subsurface conditions and they classified into proved, provable and possible reservoirs. In this study, a similar approach is used.

Table 8 presents values of proved, provable and possible reservoir volumes, porosities, temperatures and densities, considered for the Berlin geothermal area. In the area categorization, the present wellfield is taken as a proved area, the thermally altered area as a provable and the total area of geothermal activity as a possible area (ELC, 1993).

TABLE 8: Numerical values used to calculate the stored heat in the Berlin reservoir

Parameter	Proved	Provable	Possible
Area (km^2)	2	8	20
Thickness (m)	1000	1000	1000
Porosity (%)	10	9	6
Temperature (°C)	300	290	250
Rock density (kg/m^3)	2600	2600	2600
Specific heat	.85	.85	.85

In order to obtain a rough estimation for the recovery factor for the Berlin field, the system was considered closed and the total mass and the possible heat yield estimated for a chain of conditions. Initially, the reservoir is considered liquid saturated with 120 bar-a pressure (P_1). The liquid state remains until the reservoir reaches 85 bar-a (P_2) which is the saturation pressure of water at 300°C. The mass withdrawn through this state is estimated as

$$M = V\rho_w[\phi c_w + c_r(1-\phi)](P_1 - P_2)$$

Substituting values only for the provable area, and considering compressibilities of water (c_w) and rock (c_r) as $3.0\text{x}10^{-9}$ and $0.7\text{x}10^{-9}$ respectively; the mass withdrawn (M) and heat yielded (Q) will be

$$M = 1.45\times10^{10}\ kg, \qquad Q = 19.5\times10^{12}\ kJ$$

During the next production stage the reservoir is believed to produce only steam as all the separated fluid is to be injected. These conditions are maintained down to 40 bar-a pressure which is the estimated minimum reservoir pressure that allows discharge from the wells. This value is a rough estimation and was not obtained from pressure decline analysis. At this time the reservoir steam saturation, S, is given by

$$S = 1 - [C_r\rho_r(1-\phi)(T_1 - T_2) + \phi\rho_{w1}(h_{w1} - h_{s2})] / [\phi\rho_{w2}(h_{w2} - h_{s2})]$$

where the subscripts $_{1,2}$ refer to saturation values at 85 and 40 bar-a respectively.

Substituting values into the above equation gives a saturation of 0.24. This gives for the withdrawal of steam during the boiling phase

$$M_s = V\phi[\rho_{w1} - (S\rho_{s2} + (1-S)\rho_{w2})] = 0.044\times10^{12}\ kg$$

The heat yielded through this process is 138.5×10^{12} kJ. The value of the recovery factor follows as:

$$R_f = \frac{Total\ heat\ yield}{Heat\ available} = \frac{158\times10^{12}}{1.545\times10^{15}} = 0.102$$

The recovery factor calculated by this way is close to the following relationship:

$$R_f = 1.25\,\phi$$

given that ϕ is close to 10% in the wellfield, as measured in the core data.

For electrical purposes, an additional conversion efficiency factor must be used in order to convert the thermal energy into electricity. The Ahuachapan power plant had a thermal efficiency of 0.09 during the last 10 years. The same value is believed to be applicable for the Berlin field. Additional load factor of 0.8 is assumed and 30 year life period for the power plant.

The following equation applies for the electrical energy available and Table 9 shows the final result.

$$MW_e = \frac{\textit{Thermal energy} \times \textit{recovery factor} \times \textit{thermal efficiency}}{\textit{load factor} \times 30\ \textit{years} \times 3.15 \times 10^{10}}$$

TABLE 9: Available electrical energy for the Berlin reservoir by volumetric analysis

Area	R_f	MW_e
Proved	0.125	9
Provable	0.112	27
Possible	0.075	29
Total	-	65

Table 9 resulted in a total of 65 MW_e for 30 years of plant operation and the recovery factor obtained is between 0.075 to 0.125. The capacity for the present wellfield is 9 MW_e which is considerably lower than in Ahuachapan. The Ahuachapan wellfield has an area of 1.5 km^2 and is still producing an average of 50 MW_e after 25 years. This indicates that a recovery factor higher than 0.125 should be expected in the Berlin field.

6.2 Lumped model simulation

In order to obtain additional information about the potential of the Berlin field, a lumped model simulation was carried out. For that purpose the programme LUMPFIT was used to match the pressure interference data collected during 14 months of production from the field.

In the lumped model analysis, several properties of the geothermal system are lumped into a few parameters for a simple match between observed and calculated data. Its basic concern is the quantitative relationship between input and output of the system regardless of the actual physical properties (Axelsson, 1985). The main advantages of lumped models are their simplicity and the fact that they require relatively little time and are inexpensive. This kind of analysis is especially applicable to cases where a limited number of wells have been drilled, and some pressure transient data is available.

The programme LUMPFIT, used for this purpose, was developed by Axelsson and Arason at Orkustofnun. The theoretical background is given by Axelsson and Bodvarsson (1987) and Axelsson (1985; 1989). LUMPFIT simulates pressure response data from liquid-dominated reservoirs, and is based on an automatic non-linear least square iterative inverse technique. This programme considers a general lumped network consisting of N storage tanks that simulate the reservoir or recharge areas, with mass storage coefficients κ. The tanks are serially connected by resistors of conductivity σ.

To simulate pressure response data from a liquid dominated reservoir, an appropriate and best fitting lumped model with parameters σ and κ must be chosen (Axelsson and Arason, 1992). Figure 37 shows the model that is supposed to give a best match to the measured data and Figure

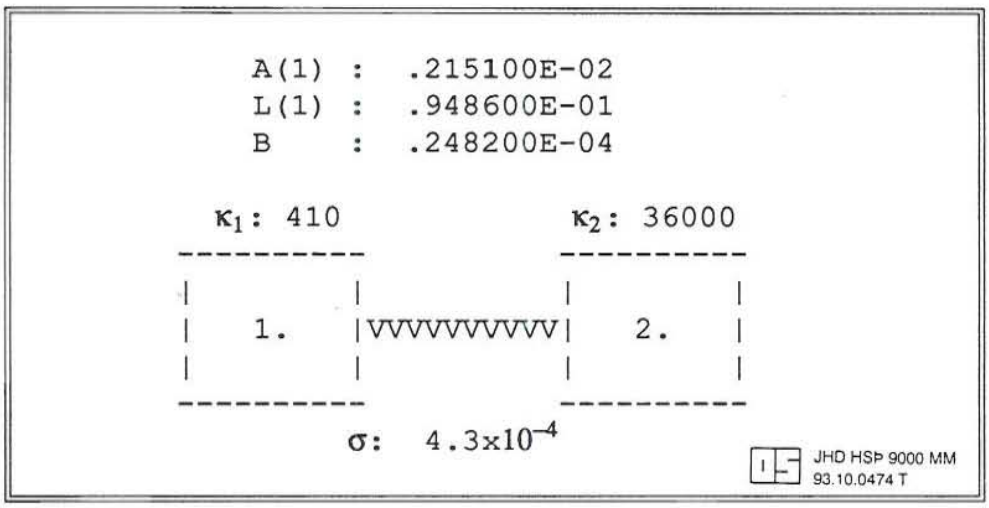

FIGURE 37: A lumped, double tank model for the Berlin reservoir

38 shows the match between measured and calculated pressures. It should be noted that only the net mass production from the field was considered for this simulation, equal to the total mass produced by TR-2 minus the injected mass in TR-9 and TR-1.

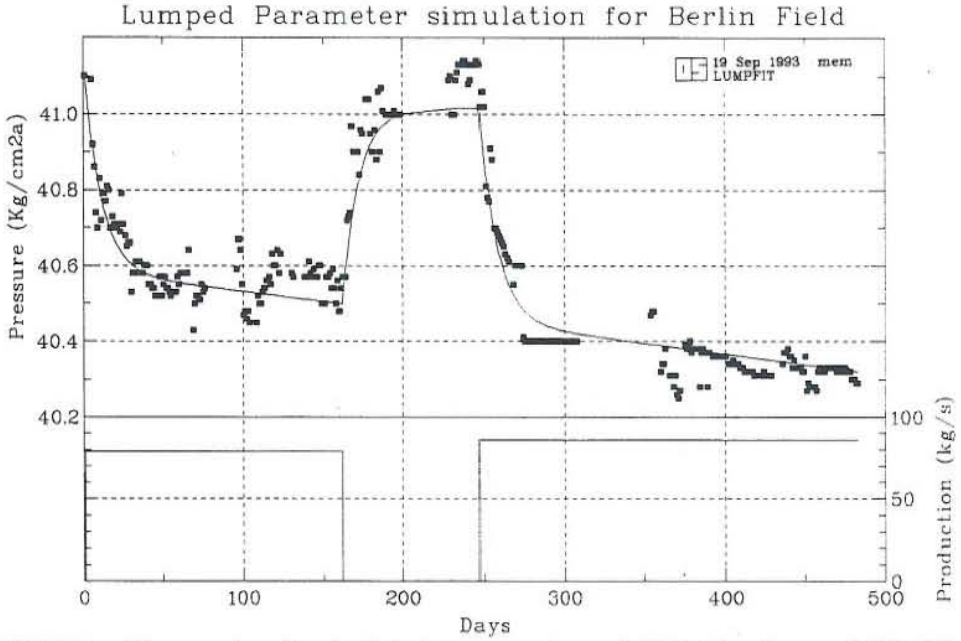

FIGURE 38: Observed and calculated pressure in well TR-4 by the model in Figure 37

Assuming a closed system of no boiling (free surface), one can convert the storage coefficients κ into reservoir volumes (Axelsson, 1993) as

$$\kappa = V\rho_w c_t = V\rho_w[\phi c_w + c_r(1-\phi)]$$

Solving for porosity equal to 10% and reservoir temperature 300°C, gives a volume of 0.30 and 26 km^3 for the κ_1 and κ_2 tanks respectively. If the reservoir thickness is believed to be 1000 m, the areas are 0.30 and 26 km^2. Therefore, an area close to 30 km^2 is perhaps a good reservoir area estimation, as was considered in Table 5.

The average permeability of the wellfield can also be estimated by the lumped parameters, considering a 2-D radial symmetry model. This model considers two concentric cylinders of volumes V_1 and V_2, estimated above. The conductivity is then given as (Axelsson, 1993):

$$\sigma = \frac{2\pi h}{\ln(\frac{r_2}{r_1})} \frac{k}{\nu}$$

where

h	- reservoir thickness	r_1	- half radius of the inner cylinder,
r_2	- half radius of the outer cylinder	k	- average permeability
ν	- kinematic viscosity μ/ρ		

Solving for r_1 and r_2 by using the previous reservoir volume estimates and thickness, gives permeability values ranging up to 25 mD, compared with 40 to 60 mD as calculated in the VARFLOW analysis (Chapter 3.5). This difference is reasonable, considering the various assumptions made to achieve these results.

6.3 Volumetric assessment by the Monte Carlo probability method

The previous study of the power potential of the Berlin reservoir shows that high uncertainty is included in several of the factors that serve as a base for the computations. In order to include this uncertainty into the computations, a method called Monte Carlo volumetric assessment has been proposed (Sarmiento, 1993). The basic equation of power output is the same as in Chapter 6.1, but this time a random probability is assigned to some of the reservoir properties in that equation. Table 10 shows the properties used here (considering only squared probability distribution).

TABLE 10: Numerical values of the Berlin reservoir properties used for the Monte Carlo volumetric assessment

Property	Units	From	To
Porosity	%	7	12
Area	km^2	5	10
Thickness	m	2000	3000
Rock density	kg/m^3	2600	2600
Rock heat capacity	J/kg/°C	0.85	0.85
Reservoir temperature	°C	250	300
Reference temperature	°C	180	180
Water density	kg/m^3	722	722
Water enthalpy at reservoir temp.	kJ/kg	1085	1345
Water enthalpy at reference temp.	kJ/kg	763	763
Recovery factor ratio		1.25 ϕ	
Thermal efficiency ratio		0.09	
Load plant factor		0.80	
Plant life period	years	30	
Conversion factor to MW_e		3.15×10^{10}	

A total of 1000 computations were made using the equations from Chapter 5.1 in a spread sheet (QPRO). Figure 39 presents the results. As seen in the figure, production rates up to 60 MW_e are very probable according to the study.

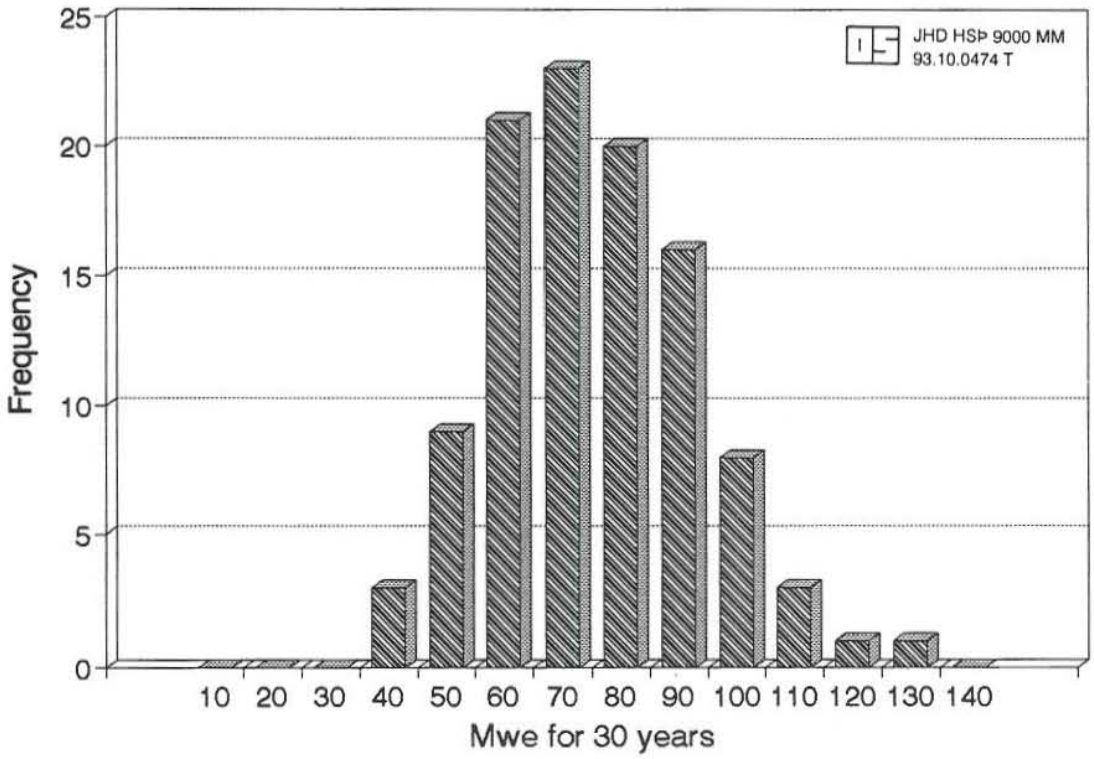

FIGURE 39: The power potential of the Berlin field
by Monte Carlo volumetric assessment

7. CONCLUSIONS AND RECOMMENDATIONS

The main conclusions of this report are:

a. The geoscientific information indicates that the subsurface flow paths in the Berlin area, are controlled by two main fault systems oriented NNW-SSE and NE-SW. A recharge zone of ≥ 300°C liquid water is assumed at great depths at the central part of the Berlin caldera. The flow from this source follows the northeast trending caldera rim towards the wellfield, where a change in flow direction to the northnorthwest is expected. This is due to the NNW-SSE directing faults seen in the region.

b. The Berlin reservoir is composed of two reservoirs; a shallow one, located close to sea level, with temperatures around 230°C, and a deeper one at -1000 m a.s.l. with temperatures close to 300°C. The temperature distribution in both reservoirs is characterized by lateral flow, which may be due to the combined influence of northeast trending faults and horizontally permeable formations.

c. The well test analysis suggests a large, liquid dominated reservoir with permeability between 50-100 mD and high storativity. The reservoir is furthermore assumed to be close to boiling condition during production as is indicated by wellbore simulations. This may lead to the formation of a two-phase zone within the deep reservoir during long term production.

d. The natural state pressure and temperature data can be simulated with a 3-D numerical model, using the TOUGH numerical code. This model gives satisfactory results after 100,000 years of steady inflow of 30 kg/s and 1400 kJ/kg enthalpy.

e. In order to simulate the minor drawdown seen in the production data, a large reservoir volume was needed. Another reason for the reservoir's high storativity, not considered here, might be boiling in the reservoir, possibly at shallow depths.

f. The constructed model is sensitive to the caprock layer permeability, but less sensitive to permeability changes in the deep reservoir. A strong coupling effect was observed between the deep inflow rate and the caprock permeability distribution.

g. No performance calculations are shown by using the numerical model. This has to do with the several coarse assumptions that were made during the development of the model, and with the limited production data available to simulate.

h. A general reservoir assessment by using volumetric calculations, lumped model and the Monte Carlo volumetric probability method, suggests that the possible power potential for the Berlin geothermal field is between 60 and 80 MW_e.

It is questionable whether the geothermal research in the Berlin field has led to a secure foundation for deciding the size of a condensing power plant. Although most of the available data show positive results, it should be kept in mind that negligible production has taken place from the reservoir. The production data, on the other hand, often provides information about critical reservoir properties, like the reservoir volume and its response to production.

The following list suggests some items that may lead to more accurate results from numerical simulation studies. They are:

1. More geological information, mainly geophysical, in order to determine the size and boundaries of the deeper reservoir, the locations of flow paths through the outer part of the caldera rim and perhaps the connection between the shallow and the deep reservoir.

2. Flowing surveys in the Berlin wells will contribute to the knowledge of the thermodynamic condition of the Berlin reservoir, especially if a localized well drawdown will lead to boiling in the reservoir.

3. Additional pressure transient tests might provide important information about the transmissivity and storativity of the reservoir. This data could for example be collected from pumping tests conducted during well completion.

4. The numerical model, used in this report, suggests a large volume for the single-phase liquid reservoir. Careful analysis of temperature and pressure in the shallow reservoir and in the caprock might show that the geothermal reservoir has a free surface, explaining the high storativity observed and providing a different approach to modelling the field.

5. An inspection of discharge rates from hot springs and fumaroles provides additional information about mass flow from the system. This is to be used for constraining later natural state modelling.

ACKNOWLEDGEMENTS

I am grateful to the staff of UNU and Orkustofnun, most specially to Dr. Ingvar Birgir Fridleifsson, for the award of the 1993 Geothermal Training Programme Fellowship.

I sincerely thank Mr. Grimur Bjornsson, my adviser, for sharing his experience and knowledge on different reservoir engineering subjects as well as supervising this work, and for his untiring support during our stay in Iceland.

Special thanks go to Dr. Thordur Arason for his assistance and patient guidance during our simulation work.

I would also like to extend my thanks to Mr. Ludvik S. Georgsson for his help and assistance and thanks also to Ms. Margret Westlund for correcting this work.

I would also express my gratitude to the Comisión Ejecutiva Hidroeléctrica del Rio Lempa (CEL), specially to the Superintendecia de Explotación Geotérmica for giving me the chance to participate in this seminar and also by providing me with all the necessary information used in this work.

Finally, I would like to express my gratitude to the more important persons of my life: my wife Lilian Hate, and my daughters Laura Aracely, Luisa Alejandra and Liliana Aydee for their understanding and spiritual support during these six months of physical separation.

REFERENCES

Axelsson, G., 1985: Hydrology and thermomechanics of liquid-dominated hydrothermal systems in Iceland. Ph.D. thesis, Oregon State University, Corvallis, Oregon, 192 pp.

Axelsson, G., 1989: Simulation of pressure response data from geothermal reservoir by lumped parameter models. Proceedings, 14th Workshop on Geothermal Reservoir Engineering, Stanford University, Cal., 257-263.

Axelsson, G., 1993: Geothermal reservoir engineering. UNU G.T.P., Iceland, unpublished lecture notes.

Axelsson, G., and Arason, P., 1992: LUMPFIT automated simulation of pressure changes in hydrogeological reservoir. Version 3.1, User's guide. Orkustofnun, Iceland.

Axelsson, G., and Bodvarsson, G., 1987: Analysis of production data from a fracturated liquid-dominated geothermal reservoir in Iceland. Geothermal Resources Council, Transactions, 11, 575-580.

Banwell, C., 1963: Thermal energy from the earth's crust - Introduction and part I. J. Geology and Geophysics, 6, 52-69.

Bjornsson, G., and Bodvarsson, G., 1987: A multifeedzone wellbore simulator. Geothermal Resources Council, Transactions, 11, 503-507.

Bodvarsson, G., 1974: Geothermal resources energetics. Geothermics, 3, 82-92.

Bodvarsson, G., O'Sullivan, M., and Tsang, C., 1986: Modelling of geothermal systems. J. Petr. Eng., 38., report LBL-18268.

CEL, 1990: Volcanology synthesis of the Berlin geothermal field. CEL report, July 1990 (in Spanish).

CEL, 1991: Superficial geochemistry synthesis of the Berlin geothermal field, CEL report, February 1991 (in Spanish).

CEL, 1993: The Berlin wells, data summary. CEL report, March 1993 (in Spanish).

Electroconsult - ELC, 1982: First geothermal power plant in the eastern side of El Salvador. Final report submitted to CEL in November 1982 (in Spanish).

Electroconsult - ELC, 1993: An outline report of the Berlin field. Preliminary report submitted to CEL in May 1993 (in Spanish).

Lawrence Berkeley Laboratory, 1982: Low-to-moderate temperature reservoir engineering handbook, VARFLOW user's manual, Vol. II, report IDO-10099.

Lawrence Berkeley Laboratory, 1991: The Ahuachapan geothermal field exploitation model, performance predictions, economics analysis, May 1991, report LBL-31132.

Mufler, P., and Cataldi, R., 1977: Methods for regional assessment of geothermal resources. ENEL-ERDA Agreement, part 1, 131-207.

Nathenson, M., 1975: Physical factor determining the fraction of stored energy recoverable from hydrothermal convection systems and conduction-dominated areas. U.S. Geological Surveys, open-file report 75-525, 38 pp.

Nathenson, M., and Mufler, L., 1975: Geothermal resources in hydrothermal convection systems and conduction-dominated areas. In: White, D.E., and Williams, D.L., (editors), Assessment of Geothermal Resources of the United States, 1975. U.S. Geological Surveys, circular 726, 104-121.

Pruess, K., 1987: TOUGH User's guide. Lawrence Berkeley Laboratory, report LBL-20700, 75 pp.

Sarmiento, Z., 1993: Geothermal development in the Philippines. UNU G.T.P., Iceland, report 2, 99 pp.